

Geometric Operator Quantum Speed Limit, Wegner Hamiltonian Flow and Operator Growth

Niklas Hörnadel¹, Nicoletta Carabba¹, Kazutaka Takahashi^{1,2}, and Adolfo del Campo^{1,3}

¹Department of Physics and Materials Science, University of Luxembourg, L-1511 Luxembourg, G. D. Luxembourg

²Department of Physics Engineering, Faculty of Engineering, Mie University, Mie 514-8507, Japan

³Donostia International Physics Center, E-20018 San Sebastián, Spain

Quantum speed limits (QSLs) provide lower bounds on the minimum time required for a process to unfold by using a distance between quantum states and identifying the speed of evolution or an upper bound to it. We introduce a generalization of QSL to characterize the evolution of a general operator when conjugated by a unitary. The resulting operator QSL (OQSL) admits a geometric interpretation, is shown to be tight, and holds for operator flows induced by arbitrary unitaries, i.e., with time- or parameter-dependent generators. The derived OQSL is applied to the Wegner flow equations in Hamiltonian renormalization group theory and the operator growth quantified by the Krylov complexity.

In what time scale does a physical process unfold? Time-energy uncertainty relations have long been used to estimate characteristic time scales in physical processes, including lifetimes in quantum decay, tunneling times, and the duration of a quantum jump, among others [1–4]. In the quantum domain, Mandelstam and Tamm put the time-energy uncertainty relation on firm ground in their 1945 work [5]. They provided its rigorous derivation by combining the Heisenberg equation of motion and the Robertson uncertainty relation. They went a step further by identifying the minimum time for the quantum state of a system to evolve into a distinct state, using the energy dispersion of the initial state as an upper bound to the speed of evolution. In doing so, they introduced an early example of a quantum speed limit (QSL).

Over the last decades, such an approach has been refined and generalized to a great extent [6, 7]. Margolus and Levitin found an alternative bound to the speed of evolution in terms of the mean energy of the system [8], and ensuing works showed that an infinite family of bounds exist in terms of other moments of the generator of evolution [9, 10]. QSLs have also been derived for time-dependent Hamiltonians [11–13], open systems described by master equations [14–17], and with a stochastic evolution under continuous quantum measurements [18]. They have been further extended to the classical domain, with applications ranging from Hamiltonian dynamics to stochastic thermodynamics [19–25]. QSLs generally involve a notion of distance between quantum states and an upper bound to the speed of quantum evolution. While the Bures angle, defined in terms of the Uhlmann fidelity [26], is often the default choice for the distance between quantum states, other

alternatives can provide tighter QSLs [17, 27–29]. This freedom is particularly important in the context of many-body systems given the orthogonality catastrophe and the growth of the Hilbert space with the system size [30–34].

The emphasis on quantum state distinguishability was a key stepping stone in developing QSLs. Today, QSLs find manifold applications in quantum metrology and parameter estimation [35–38], quantum control [39–42], and quantum thermodynamics [43, 44], among other fields. However, certain phenomena are naturally described in terms of operator flows, i.e., the continuous evolution of an operator according to given equations of motion. A typical example is the description of quantum evolution in the Heisenberg picture, but the relevance of operator flows is not restricted to quantum dynamics in rotating frames. Operator flows naturally arise in the Wegner flow equations for Hamiltonian renormalization [45–49], the study of operator growth and quantum complexity [50–54], and correlation functions [55], to name some examples.

Motivated by these applications, we have introduced the notion of QSL for operator flows in Ref. [56], which we shall term Operator QSL (OQSL) hereafter. Another approach pursuing QSLs for observables was proposed in [57]. At variance with conventional QSLs, OQSLs involve a notion of distance between operators (instead of quantum states) and an upper bound on the corresponding speed of evolution. OQSLs have proved useful in characterizing the time evolution of autocorrelation functions, setting bounds on dynamical susceptibilities arising in linear response theory, and the precision in parameter estimation with thermal quantum systems [56]. However, in their current form, OQSLs are restricted to flows associated with a constant generator, i.e., one that is independent of time or the relevant parameter characterizing the evolution. In addition, OQSLs lack in their present formulation an intuitive geometric description, common in other bounds arising in quantum information geometry, such as the Mandelstam-Tamm QSL.

In this work, we introduce an OQSL valid under unitary dynamics generated by a time- (or parameter-) dependent generator, that can be a generic operator or an observable, e.g., a Hamiltonian. The resulting bound admits a geometric interpretation and is shown to be tight. We illustrate its usefulness in the study of Wegner flow equations in the theory of Hamiltonian continuous renormalization group [46–48]. We characterize the OQSL for the Hamiltonian flow in detail and illustrate the possibility of saturating it when the flow of Hamiltonian parameters is described by the Toda equations. We further apply the new OQSL to the problem of operator growth in unitary quantum dynamics in Krylov space, i.e., as characterized by the Krylov complexity [54, 58–62]. We close with a discussion and an outlook pointing out directions for further work.

1 Motivation

In quantum physics, a broad class of time-correlation functions is defined through a positive semi-definite inner product. Consider any operator A evolving unitarily according to $\dot{A}_t = i\mathbb{L}A_t$, where $\mathbb{L} = [H, \cdot]$ is the Liouvillian superoperator. One class of time-correlation functions that have been considered in the literature takes the form $C(t) = (A|A_t)$, defined with the help of a Hermitian bilinear form in the space of operators,

$$(A|B) = \text{Tr}(A^\dagger \rho_1 B \rho_2). \quad (1)$$

The operators ρ_1 and ρ_2 are in general positive semi-definite, commute with the Hamiltonian, and need not have unit trace. A familiar example of this type of correlation function is obtained by setting $\rho_1 = \rho_2 = \mathbb{1}$. Eq. (1) reduces then to the Hilbert-Schmidt inner product. Another familiar instance corresponds to the choice of the identity $\rho_1 = \mathbb{1}$ and the canonical Gibbs state $\rho_2 = e^{-\beta H}/Z$ at inverse temperature β , with partition function $Z = \text{Tr } e^{-\beta H}$. Note that in general, the bilinear form in (1) is not positive definite, which means that it does not always define an inner product; instead, it will define a positive semi-definite inner product.¹ As a result, there might exist cases in which $A \neq 0$ and $(A|A) = 0$ are simultaneously fulfilled. Another example of a correlation function defined through a positive semi-definite inner product, i.e. $C(t) = (A|A_t)$, is given by the so-called Kubo inner product [55, 63–65]

$$(A|B) = \frac{1}{\beta} \int_0^\beta d\lambda \langle e^{\lambda H} A^\dagger e^{-\lambda H} B \rangle_\beta - \langle A^\dagger \rangle_\beta \langle B \rangle_\beta. \quad (2)$$

Here, $\langle \cdot \rangle_\beta$ denote the thermal expectation value and β is once again the inverse temperature.

The function $\|A\| = \sqrt{(A|A)}$ is a seminorm and we note that the condition $\|A_t\| = \|A\|$ is satisfied in the above examples for all t .² We might then ask, given a unitary flow induced by a possibly time-dependent Hamiltonian H , what is the minimal time τ for an initial observable A to reach some specific value of $C(t)$ provided that $\|A_t\| = \|A\|$ is satisfied during the whole evolution? What follows is a derivation of a speed limit that lower bounds this minimum time.

2 An Operator Quantum Speed Limit

The complex Hilbert space \mathcal{H} used to model the system will be assumed throughout this paper to be finite-dimensional. We define \mathcal{B} to be the space of linear operators acting on this space. Moreover, let $\text{End}(\mathcal{B})$ be the space consisting of all vector space endomorphism of \mathcal{B} . This linear space is commonly referred to as the Liouville space in the literature [66, 67] and its elements are referred to as superoperators.

Positive semi-definiteness of $(\cdot|\cdot)$ makes it possible for $C(t)$ to be constant for certain paths A_t even though the operator is changing in time. We will see that there is a way of “carving away” the degrees of freedom in \mathcal{H} that do not contribute to changes in $C(t)$. In doing so, we obtain an effective Hilbert subspace \mathcal{H}_P , where the restriction of $(\cdot|\cdot)$ onto this subspace defines a proper inner-product. We will see that the condition $\|A_t\| = \|A\|$ implies that A_t will be situated on a sphere centered at the origin in \mathcal{H}_P with radius $\|A\|$. This observation will then enable us to derive a geometric OQSL.

2.1 Construction of the effective Hilbert space

We let $\langle \cdot, \cdot \rangle_H$ denote the Hilbert-Schmidt inner product on \mathcal{B} . It can be shown that any positive semi-definite inner product $(\cdot|\cdot)$ can be expressed as $(\cdot|\cdot) = \langle \cdot, \mathcal{P} \cdot \rangle_H$, where \mathcal{P} is

¹We use the convention that an inner product must satisfy positive-definiteness, be linear in the second argument and conjugate symmetric

²A seminorm fulfills all the properties of regular norm except that non-zero vectors can have norm 0.

a positive semi-definite superoperator with respect to the Hilbert-Schmidt inner product. This superoperator will be unique, provided that $(\cdot|\cdot)$ has been specified—see Appendix A. As we prove in Appendix B, a useful relation between $(\cdot|\cdot)$ and \mathcal{P} is that

$$\|A\| = 0 \iff \mathcal{P}A = 0. \quad (3)$$

Since \mathcal{P} is self-adjoint, it follows from the spectral theorem that the linear space \mathcal{B} can be expressed as a direct sum of the eigenspaces of \mathcal{P} [68]. Consequently, the image of \mathcal{P} will be spanned by the eigenvectors corresponding to non-zero eigenvalues, and we thus have that $\mathcal{B} = \text{im}(\mathcal{P}) \oplus \ker(\mathcal{P})$, where $\text{im}(\mathcal{P})$ and $\ker(\mathcal{P})$ are the image and kernel of \mathcal{P} respectively. Relation (3) then implies that the restriction of $(\cdot|\cdot)$ to $\text{im}(\mathcal{P})$ will be positive definite and will thus define an inner product on the Hilbert space defined by $\mathcal{H}_{\mathcal{P}} = \text{im}(\mathcal{P})$. We will express this inner product with the usual bracket notation $\langle \cdot, \cdot \rangle$.

For any operator $A \in \mathcal{B}$, we will let $\hat{A} \in \mathcal{H}_{\mathcal{P}}$ denote the orthogonal projection of A onto $\mathcal{H}_{\mathcal{P}}$.³ More explicitly, given the spectral decomposition $\mathcal{P} = \sum_k p_k \Pi_k$, where p_k are the non-zero eigenvalues of \mathcal{P} and Π_k are the corresponding eigenprojections, we have that $\hat{A} = \sum_k \Pi_k A$. We show in Appendix C that

$$(A|B) = \langle \hat{A}|\hat{B} \rangle \quad \forall A, B \in \mathcal{B}. \quad (4)$$

An important consequence of (4) is that $C(t) = \langle \hat{A}|\hat{A}_t \rangle$. This means that if we are interested in how $C(t)$ changes over time, then we only need to consider the projected dynamics $\hat{A}(t)$ of $A(t)$.

2.2 Deriving the speed limit

If d is the complex dimension of the Hilbert space $\mathcal{H}_{\mathcal{P}}$, then we can view it as a real vector space isomorphic to \mathbb{R}^{2d} . We endow this space with the Riemannian metric given by the real part of the inner product $\langle \cdot, \cdot \rangle$. The condition that $(A|A) = (A_t|A_t)$ holds for all $t \in [0, \tau]$ then means that \hat{A}_t will be situated on the $(2d - 1)$ -dimensional sphere $\mathcal{S}_{\|A\|}$ with radius $\|A\|$ centered at the origin. The shortest path connecting two points on the sphere lies on a great circle with a distance given by the angle between the points times the radius. In other words, if \hat{A} and \hat{B} are two operators on the sphere with radius $\|A\|$, then the geodesic distance is given by

$$\text{dist}(\hat{A}, \hat{B}) = \|A\| \arccos\left(\frac{\text{Re}(A|B)}{\|A\|^2}\right). \quad (5)$$

The length of any curve \hat{A}_t on the sphere must be greater or equal to the geodesic distance. As a consequence, we obtain an operator quantum speed limit τ_{QSL} by noting that

$$\tau = \frac{\text{length}([\hat{A}_t])}{\frac{1}{\tau} \text{length}([\hat{A}_t])} \geq \frac{\text{dist}(\hat{A}_0, \hat{A}_\tau)}{\frac{1}{\tau} \text{length}([\hat{A}_t])}, \quad (6)$$

where $\text{length}([\hat{A}_t]) = \int_0^\tau \|\mathbb{L}_t A_t\| dt$ is the length of the evolution. More explicitly, the speed limit can be written in terms of $C(t)$ as

$$\tau \geq \tau_{\text{QSL}}, \quad \tau_{\text{QSL}} = \frac{\sqrt{C(0)} \arccos\left(\text{Re} \frac{C(\tau)}{C(0)}\right)}{\mathcal{V}_\tau}, \quad (7)$$

³By orthogonal, we mean orthogonality measured by the Hilbert-Schmidt inner product.

where $\mathcal{V}_\tau = \frac{1}{\tau} \int_0^\tau \|\mathbb{L}_t A_t\| dt$ is the time averaged speed of the evolution. For non-constant speeds, \mathcal{V}_τ needs in practice be replaced by an upper bound on the speed of the evolution in order to make τ_{QSL} independent on the time τ one is trying to estimate.

We stress that the speed limit τ is only guaranteed to hold whenever $\|A_t\|$ is preserved for the evolving operator. This is always satisfied in the case when $\mathcal{P} = \mathbb{1}$ so that $(\cdot|\cdot)$ becomes the Hilbert-Schmidt inner product. For more general choices of \mathcal{P} however, norm preservation will not be guaranteed to hold for all initial operators. In fact, the norm is preserved for all initial operators if and only if $[\mathbb{L}, \mathcal{P}] = 0$. Assuming $[\mathbb{L}, \mathcal{P}] = 0$, let \mathcal{P}_{nm} and $\omega_\alpha = E_n - E_m$ be the eigenvalues of \mathcal{P} and \mathbb{L} with respect to a common eigenbasis. Moreover, let A_{ij} be the components of A with respect to this basis. Define $v_\alpha = \frac{\mathcal{P}_{nm}|A_{nm}|^2}{C(0)}$, where $C(0) = \sum_{n,m} \mathcal{P}_{nm}|A_{nm}|^2$. We can then express (7) more explicitly, as

$$\tau_{\text{QSL}} = \frac{\arccos(\text{Re} \sum_\alpha v_\alpha e^{i\omega_\alpha \tau})}{\sqrt{\sum_\gamma v_\gamma \omega_\gamma^2}}, \quad (8)$$

where the indices α and γ runs from 1 to $\dim(\mathcal{H})^2$.

Example 1. In the case when $C(t) = \text{Tr}(A^\dagger A_t e^{-\beta H}/Z)$ we have that $\mathcal{P}A = Ae^{-\beta H}/Z$ and a common eigenbasis between \mathbb{L} and \mathcal{P} is given by the operators $|E_n\rangle\langle E_m|$ where the eigenvalues of \mathcal{P} are given by $\mathcal{P}_{nm} = e^{-\beta E_m}/Z$.

Example 2. For the Kubo inner-product we can view \mathcal{P} as the composition $\mathcal{P} = \mathcal{A} \circ \mathcal{B} \circ \mathcal{C}$ of the three superoperators defined by $\mathcal{A}(A) = \frac{Ae^{-\beta H}}{Z}$, $\mathcal{B}(A) = \frac{1}{\beta} \int_0^\beta d\lambda e^{-\lambda H} Ae^{\lambda H}$ and $\mathcal{C}A = A - \text{Tr}(A)\mathbb{1}$. The superoperators \mathcal{A} and \mathcal{B} commute with a common eigenbasis being given by the eigenvectors $|E_n\rangle\langle E_m|$. A speed limit for a time-evolving operator A_t using the Kubo inner-product can then be obtained by using $\tilde{A}_t = \mathcal{C}(A_t)$ and $\tilde{\mathcal{P}} = \mathcal{A} \circ \mathcal{B}$ instead of A_t and \mathcal{P} and then use that $\tilde{\mathcal{P}}_{nm} = \frac{e^{-\beta E_m}}{\beta Z} \int_0^\beta e^{\lambda(E_m - E_n)} d\lambda$ and $\tilde{A}_{nm} = A_{nm} - \sum_k A_{kk}$.

Let us note that the OQSL (7) is saturated by any traceless observable involving solely the coupling of the ground state and an excited state of a time-independent Hamiltonian, in the same spirit as the superposition of these eigenstates saturates the standard QSLs for states [69]. To show this, let us consider a time-independent Hamiltonian H and let us denote by $|0\rangle$ and $|E\rangle$ its ground state and the eigenstate with energy E : $H|0\rangle = 0$ and $H|E\rangle = E|E\rangle$. Then, it is straightforward to see that the operator $A = \frac{1}{\sqrt{2}}(|0\rangle\langle E| + |E\rangle\langle 0|)$ exactly saturates the OQSL (7) with respect to the Hilbert-Schmidt inner product $(A|B) = \text{Tr}(A^\dagger B)$. Indeed, the autocorrelation function reduces to $C(t) = \cos(Et)$, in natural units, while the velocity is constant and takes the value $\mathcal{V} = \|[H, A]\| = E$. Therefore, being $C(0) = 1$ due to the normalization, the OQSL (7) reduces to an identity at any time.

This intuition, that when the operator dynamics is confined to two time-independent Hamiltonian eigenspaces the evolution occurs along a geodesic trajectory, can be made more rigorous and general, as we shall describe below identifying the general conditions for the saturation of the OQSL (7).

2.3 Refined speed Limit

Suppose we can find a decomposition of \hat{A}_t such that $\hat{A}_t = S + V_t$, where S and V_t stays orthogonal with respect to the metric $\text{Re}\langle \cdot, \cdot \rangle$ throughout the evolution. We then have that

the minimal time it takes V to reach the operator V_τ is smaller or equal to the time it takes \hat{A} to reach \hat{A}_τ . We can thus obtain another speed limit by substituting $C(t)$ with $(V|V_t)$ in (7). Using that S and V_t are orthogonal, one can write $\text{Re}(V|V_t) = \text{Re} C(t) - \|S\|^2$. Our refined speed limit thus takes the form

$$\tau \geq \tau_{\text{REF}}, \quad \tau_{\text{REF}} = \frac{\sqrt{C(0) - \|S\|^2} \arccos\left(\text{Re} \frac{C(\tau) - \|S\|^2}{C(0) - \|S\|^2}\right)}{\mathcal{V}_\tau}. \quad (9)$$

This OQSL is a generalization of (7) since we can always trivially consider the case when $S = 0$. Also, since $\mathbb{1}$ stays invariant throughout the flow generated by the Hamiltonian, we can always consider the choice $S = (\mathbb{1}|A)\mathbb{1}$. In the particular case when $(\cdot|\cdot)$ is the Hilbert-Schmidt inner product, this choice of S reduces (9) to the speed limit, denoted by T_Θ , in [28].

What is worth noting is that the speed limit (9) becomes tighter the larger the norm of S is. We can understand this from a geometrical perspective. The speed limit is saturated whenever the traced-out curve of V_t follows a great circle on the sphere $\mathcal{S}_{\|V\|}$. This means that the evolution will be contained in a two-dimensional subspace. If we then let X and Y be a pair of orthonormal vectors spanning this subspace, we must have that $V_t/\|V\| = \cos \theta(t)X + \sin \theta(t)Y$, where $\theta(t)$ is some real-valued function of t .⁴ Given that S is non-zero, the corresponding curve of \hat{A} must then be situated on an effective Bloch sphere spanned by the operators X , Y and S .⁵ More explicitly, we have that $\hat{A} = \|V\| \cos \theta(t)X + \|V\| \sin \theta(t)Y + S$ will trace out a curve following a circle centered at S (see figure 1). Since this circle is not centered at the origin, it will not be a great circle on the sphere $\mathcal{S}_{\|A\|}$. A consequence of this is that the length of this curve must be strictly larger than the geodesic distance on $\mathcal{S}_{\|A\|}$. This length is precisely the numerator in (9) and we can thus conclude that (9) gives a strictly tighter inequality than (7). The difference between these inequalities becomes greater the larger $\|S\|$ is, which can be seen in figure 2.

Consider the case when $\ker(\mathbb{L}) \cap \mathcal{H}_P$ is invariant throughout the evolution, for example, when the Hamiltonian commutes with itself for any two points in time. We then have that the norm of S is maximal when S is equal to the orthogonal projection of \hat{A} onto the subspace $\ker(\mathbb{L}) \cap \mathcal{H}_P$ —see Appendix E.⁶ Calling this component P_0 , we thus have that the tightest possible refinement, in this case, is given by

$$\tau \geq \tau_{\text{OREF}} \geq \tau_{\text{REF}} \geq \tau_{\text{QSL}}, \quad \tau_{\text{OREF}} = \frac{\sqrt{C(0) - \|P_0\|^2} \arccos\left(\text{Re} \frac{C(\tau) - \|P_0\|^2}{C(0) - \|P_0\|^2}\right)}{\mathcal{V}_\tau}. \quad (10)$$

We will refer to this as the optimal refinement of the OQSL.

⁴In fact, if we choose X and Y so that $X = V$, then θ is the angle between V and V_t and is given by $\theta(t) = \arccos\left(\text{Re} \frac{C(t) - \|S\|^2}{C(0) - \|S\|^2}\right)$.

⁵We emphasize that the operators S , X and Y are orthogonal with respect to $\text{Re}\langle \cdot, \cdot \rangle$ and not necessarily the Hilbert-Schmidt inner product.

⁶The orthogonal projection here is with respect to the inner product $\langle \cdot, \cdot \rangle$.

$$\mathcal{S}_{\|A\|} \cap \text{span}\{S, X, Y\}$$

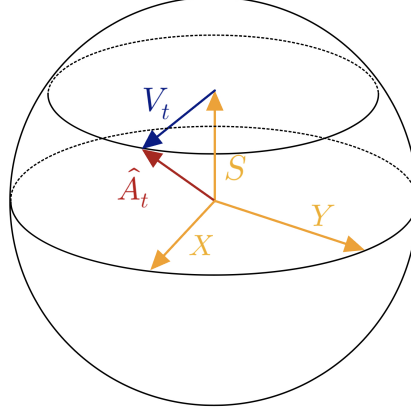


Figure 1: As the evolving operator saturates the refined speed limit, it will move along a circle that is displaced from the origin by S . As a consequence, the length of the traced-out curve will be strictly larger than the geodesic distance in $\mathcal{S}_{\|A\|}$. The numerator in (9) is exactly the length of this traced-out curve, and we can thus conclude that the refined speed limit is strictly tighter than the original one, given that $S \neq 0$.

3 More on the Conditions for Saturation

As discussed in section 2, the part of the evolution that induces a change in the time-correlation function will be situated on the sphere $\mathcal{S}_{\|A\|}$ in the effective Hilbert space \mathcal{H}_P . The OQSL (7) will then be saturated whenever the traced-out curve follows a great circle. In the case when we could find a decomposition $\hat{A}_t = S + V_t$, where S and V_t remain orthogonal, we could consider the refined speed limit (9), which is saturated if and only if V_t follows a great circle on the sphere $\mathcal{S}_{\|V\|}$. We discussed that for saturation of (9), there exists a pair of orthonormal vectors X and Y such that $\hat{A} = \|V\| \cos \theta(t) X + \|V\| \sin \theta(t) Y + S$. If we choose $X = \hat{A}/\|\hat{A}\|$, then the function $\theta(t)$ is the angle between V and V_t with respect to the real-valued inner product $\text{Re}\langle \cdot, \cdot \rangle$ and is more explicitly given by $\theta(t) = \arccos\left(\text{Re} \frac{C(\tau) - \|S\|^2}{C(0) - \|S\|^2}\right)$.

This section will discuss the conditions for saturation for two particular cases. In the first case, we consider the consequences of the operator \hat{A} having support in only two of the eigenspaces of the Hamiltonian. In the second case, we assume \hat{A} to be Hermitian, allowing us to draw connections between the saturation of the OQSLs and the dimension of an underlying Krylov space.

3.1 Evolution with support in only two eigenspaces of the Hamiltonian

Consider the case when the Hamiltonian commutes with itself at any two points in time. We will consider the case when \hat{A} has non-zero support in only two of the eigenspaces of the Hamiltonian.⁷ Let E and E' denote the energies of these two eigenspaces through time and let $\omega = E - E'$ be the energy gap. If P_E and $P_{E'}$ are the corresponding eigenspace projectors, then $\hat{A} = P_E \hat{A} P_E + P_E \hat{A} P_{E'} + P_{E'} \hat{A} P_E + P_{E'} \hat{A} P_{E'}$ and it is straight forward to check that

⁷An operator A is said to have non-zero support in a subspace $\mathcal{X} \subseteq \mathcal{H}$ if $\exists |\psi\rangle \in \mathcal{X}$ s.t. $A|\psi\rangle \neq 0$.

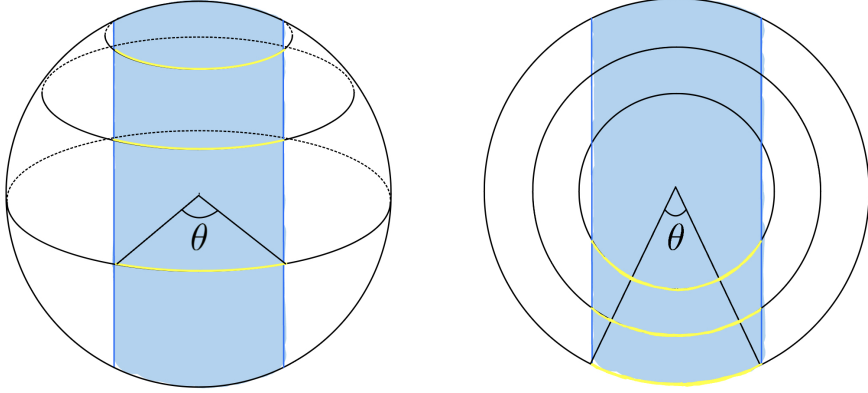


Figure 2: As $\|S\|$ grows larger, the center of the circle that \hat{A}_t follows will be closer to the poles of the sphere. Consequently, \hat{A}_t moves in a more curved path, as highlighted by the yellow segments where the right figure shows a top view of the sphere, and have to travel further in order to reach the same angle θ . The result of this is that the refined speed limit becomes increasingly tight the larger $\|S\|$ is.

$\mathbb{L}P_E\hat{A}P_{E'} = \omega P_E\hat{A}P_{E'}$, $\mathbb{L}P_E\hat{A}P_{E'} = -\omega P_{E'}\hat{A}P_E$ and $\mathbb{L}P_E\hat{A}P_E = \mathbb{L}P_{E'}\hat{A}P_{E'} = 0$. In other words, \hat{A} is spanned by the eigenspaces of the Liouvillian with eigenvalues 0, ω , and $-\omega$. Let P_0 , P_ω , and $P_{-\omega}$ be the corresponding projections of \hat{A} onto these three eigenspaces. More explicitly, we have in this specific case that $P_0 = P_E\hat{A}P_E + P_{E'}\hat{A}P_{E'}$, $P_\omega = P_E\hat{A}P_{E'}$ and $P_{-\omega} = P_{E'}\hat{A}P_E$ and we can write $\hat{A} = P_0 + P_\omega + P_{-\omega}$. The evolution of \hat{A} is given by

$$\begin{aligned}\hat{A}_t &= P_0 + e^{i \int_0^t \omega(t') dt'} P_\omega + e^{-i \int_0^t \omega(t') dt'} P_{-\omega} \\ &= P_0 + \cos\left(\int_0^t \omega(t') dt'\right) (P_\omega + P_{-\omega}) + \sin\left(\int_0^t \omega(t') dt'\right) (iP_\omega - iP_{-\omega}) \quad (11) \\ &= P_0 + \cos \theta(t) X_\omega + \sin \theta(t) Y_\omega.\end{aligned}$$

Here, we have introduced the non normalized operators $X_\omega = P_\omega + P_{-\omega}$ and $Y_\omega = iP_\omega - iP_{-\omega}$ and the angle $\theta(t) = \int_0^t \omega(t') dt'$ between $\hat{A} - P_0$ and $\hat{A}_t - P_0$. The requirement that $\|\hat{A}_t\|$ is constant in the interval $[0, \tau]$ implies that P_0 , X and Y are orthogonal and that X and Y have the same norm—see Appendix F.⁸ We can thus conclude that $\hat{A}_t - P_0$ moves along a great arc and thus saturates the optimal refined speed limit (10). One of the consequences of this is that any qubit system with a commutative Hamiltonian must satisfy the speed limit (10).

The above result can be extended to non-commuting Hamiltonians that keep the eigenspaces corresponding to E and E' invariant. One might wonder whether the Hamiltonian must keep these eigenspaces invariant for the evolving operator \hat{A}_t to achieve saturation. The answer is no. To see this, we can consider the commuting Hamiltonian H_t above and add to it any non-trivial Hamiltonian \tilde{H}_t that commutes with \hat{A}_t for all times $t \in [0, \tau]$. The Hamiltonian $H_t + \tilde{H}_t$ then generates the same path for \hat{A}_t as the Hamiltonian H_t . The difference is that $H_t + \tilde{H}_t$ will not keep the eigenspaces of E and E' invariant.

⁸Note that we never need to assume that \hat{A} is Hermitian in order to conclude this.

3.2 Relation to Krylov dimension for Hermitian operators

When \hat{A} is Hermitian, it can be illuminating to describe the saturation conditions in terms of the dimension of the Krylov space of the evolving operator \hat{A}_t . The Krylov space is defined to be the smallest subspace containing the evolution. In the Hermitian case, this is a real vector space. We can then conclude that saturation of (7) happens if and only if the dimension of the Krylov space is equal to two. Similarly, given that $S \neq 0$, we have that a necessary condition for saturation of (7) is that the dimension of the Krylov space is equal to three.

In the case when the Liouvillian is time-independent, the Krylov dimension is given by the number of eigenspaces of \mathbb{L} that \hat{A} has support in—see Appendix D. If one of these eigenspaces is the kernel of \mathbb{L} , then we can say that the bound will be saturated if and only if the Krylov dimension is smaller or equal to three.

4 Hamiltonian Flow Equations in Continuous Renormalization Group

Operator flows are ubiquitous in physics and are not restricted to time evolution. In this section, we show that the continuous renormalization group provides an arena in which Hamiltonian flows naturally occur and where OQSLs are of relevance.

As a preamble, we note that the continuous renormalization group is also extensively used in the study of the complexity of quantum states. For instance, the continuous version of the Entanglement Renormalization tensor networks, cMERA [70, 71], implements a real space renormalization in which the flow of a quantum state is described as a function of a continuous parameter characterizing the length scale. A cMERA Hamiltonian generates translations of the cMERA parameter. The use of conventional QSL has been explored in this context to investigate the complexity of states in quantum field theory [72], using the path integral description of tensor networks [73, 74]. These works result from an effort to characterize the growth of quantum complexity in quantum field theories, a context in which conventional QSLs had been applied [75, 76]. Indeed, all these results concern flows of quantum states and can thus be tackled with conventional QSL.

In this section, we consider a different framework for the continuous renormalization group as a paradigmatic example and test bed for our result, the OQSL (7). Specifically, we focus on the Hamiltonian flow formulated by Wegner [45] and Glazek and Wilson [46, 47], as a method for Hamiltonian block-diagonalization [48, 49]. Consider the Hamiltonian flow $H(l) = U(l)H(0)U(l)^\dagger$ with respect to some parameter l , where $U(l)$ is a unitary operator satisfying $U(0) = \mathbb{1}$, and $H(0)$ is the Hamiltonian of which the block diagonal form is desired. The flowing Hamiltonian satisfies the differential equation

$$\frac{dH(l)}{dl} = [\eta(l), H(l)], \quad (12)$$

where $\eta(l) = \frac{dU(l)}{dl}U(l)^\dagger$ is the l -dependent generator of the unitary flow. For specific choices of $\eta(l)$, the initial Hamiltonian $H(0)$ eventually flows to its (block)-diagonal form, thus achieving the desired diagonalization. At each point of the flow, let us define the target Hamiltonian $H_T(l)$ as the diagonal part of $H(l)$,

$$H_T(l) = \sum_n \epsilon_n(l) |n\rangle \langle n|, \quad (13)$$

where we have defined $\epsilon_n(l) \equiv H_{nn}(l)$. One instance of a generator that achieves this is $\eta = [H_T, H]$, as originally proposed in [45, 48]. We shall refer to this specific choice as the Wegner flow, for simplicity, even when any Hamiltonian flow described by (12) and converging to $H_T(l)$ is generally referred to as a Wegner flow in the literature. Clearly, the choice $\eta = [H_T, H]$ is not the only possibility and we shall consider a different choice in an example below. Let us stress that the l -dependent diagonal entries $\epsilon_n(l)$ in Eq. (13) do *not* correspond to the Hamiltonian eigenvalues unless we have reached the end of the flow $l = l_f$. In that case, the flowing Hamiltonian has been transformed into its diagonal form to coincide with the target part, $H(l_f) = H_T(l_f)$. The final l_f is typically reached as $l \rightarrow \infty$, as shown explicitly in the practical example below.

By applying our general result (7) to the evolution (12), with $t \rightarrow l$, $A_t \rightarrow H(l)$ and $H(t) \rightarrow -i\eta(l)$, we obtain the following OQSL on the Hamiltonian flow

$$l \geq l_{\text{QSL}}, \quad l_{\text{QSL}} = \frac{\|H\| \arccos \frac{(H(0)|H(l))}{\|H\|^2}}{\mathcal{V}_l}, \quad (14)$$

where the speed, averaged over the interval $[0, l]$, is given by

$$\mathcal{V}_l = \frac{1}{l} \int_0^l \|[\eta(t), H(t)]\| dt. \quad (15)$$

For the rest of this section, we will only consider the case when $(\cdot|\cdot)$ is the Hilbert-Schmidt inner product. In this case we have that $\|[\eta, H]\| = \text{Tr}([\eta, H]^2)$.

4.1 Dephasing-like Wegner flow

Before applying the OQSL (14) in an explicit example, we show that the Wegner flow, although unitary, features formal similarities with a dephasing evolution, under which the off-diagonal entries of the density matrix $\rho(t)$ decay and the fixed point is set by its diagonal part only. The crucial difference is that in the Wegner flow, the diagonal part evolves as well, and it does so in such a way that the total evolution is unitary and the final diagonal form coincides with the diagonalized initial Hamiltonian. Here we aim to characterize the decay of the off-diagonal elements $H_{nm}(l)$ with $n \neq m$ and reveal its formal analogy with dephasing. To this end, let us adopt the approach of vectorization [77] and represent an operator $A = \sum_{n,m} A_{nm} |n\rangle \langle m|$ as a normalized vector

$$|A\rangle = \frac{1}{\|A\|} \sum_{n,m} A_{nm} |n, m\rangle, \quad (16)$$

where $|n, m\rangle = |n\rangle \otimes |m\rangle$ and the normalization factor has been introduced to enhance the comparison with the evolution of a quantum state ρ . Now, since we are interested in the decay of the off-diagonal elements, let us introduce the (super)projector \mathbb{Q} over the non-diagonal part of the Hamiltonian,

$$\mathbb{Q} = \mathbb{1}_{\mathcal{B}} - \mathbb{P}_{H_T}, \quad (17)$$

where $\mathbb{1}_{\mathcal{B}}$ is the identity on the operator space \mathcal{B} and \mathbb{P}_{H_T} is the (super)projector over the target Hamiltonian

$$\mathbb{P}_{H_T} = |H_T\rangle \langle H_T| = \frac{1}{\|H_T\|^2} \sum_{n,m} \epsilon_n \epsilon_m |n, n\rangle \langle m, m|. \quad (18)$$

From this expression, it follows that $\mathbb{P}_{H_T} |H_T\rangle = |H_T\rangle$ and $\mathbb{Q}|H_T\rangle = 0$. To characterize the dephasing-like decay realized by the Wegner flow, let us consider the overlap between the flowing Hamiltonian and its non-diagonal part

$$\mathcal{A}_Q(l) \equiv \langle H(l) | \mathbb{Q} | H(l) \rangle, \quad (19)$$

which quantifies how far $H(l)$ is from being diagonal and vanishes as $l \rightarrow l_f$, that is as $H(l) \rightarrow H_T(l)$. By substituting Eqs. (17) and (18) we obtain

$$\mathcal{A}_Q(l) = 1 - \frac{\|H_T\|^2}{\|H\|^2}, \quad (20)$$

where we stress that $\|H_T\|^2 = \sum_n \epsilon_n^2(l)$ depends on l . The quantity \mathcal{A}_Q identically vanishes at the end of the flow, when the Hamiltonian is diagonalized and $H(l) = H_T(l)$. Remarkably, if we choose the Wegner generator to be $\eta = [H_T, H]$ [48], then \mathcal{A}_Q decays monotonically. Indeed, its decay rate reads as

$$\frac{d}{dl} \mathcal{A}_Q(l) = -\frac{1}{\|H\|^2} \frac{d}{dl} \sum_n \epsilon_n^2 = \frac{1}{\|H\|^2} \frac{d}{dl} \sum_{n \neq m} |H_{nm}|^2, \quad (21)$$

where the last inequality follows from the conservation of the total norm, $\frac{d}{dl} \|H\| = 0$. If $\eta = [H_T, H]$ [48], it is straightforward to compute that

$$\frac{dH_{nm}}{dl} = \sum_k (\epsilon_n + \epsilon_m - 2\epsilon_k) H_{nk} H_{km} \quad (22)$$

and therefore

$$\frac{d}{dl} \mathcal{A}_Q(l) = -\frac{2}{\|H\|^2} \sum_{n,m} (\epsilon_n - \epsilon_m)^2 |H_{nm}|^2 < 0. \quad (23)$$

As a result, the overlap (19), quantifying how far we are from the target, is monotonically decreasing during the flow. This feature suggests an analogy with the well-known model of dephasing, where the purity is found to decrease monotonically [78], in a similar manner as in Eq. (23). To show this, let us consider the case of pure dephasing

$$\frac{d\rho}{dt} = -[X, [X, \rho]], \quad (24)$$

where X is a time-independent Hermitian operator satisfying $X|n\rangle = x_n|n\rangle$. Then it can be shown [78] that the purity $\text{Tr} \rho^2$ decreases monotonically with time as

$$\frac{d \text{Tr} \rho^2}{dt} = -2 \sum_{nm} (x_n - x_m)^2 |\rho_{mn}|^2. \quad (25)$$

Now, Eq. (23) can be also expressed as a ‘‘purity’’-decay of the off-diagonal Hamiltonian $H_{\text{off-diag}}(l) = H(l) - H_T(l)$ and it reads as

$$\frac{d \text{Tr} H_{\text{off-diag}}^2}{dl} = \frac{d}{dl} \sum_{i \neq j} |H_{ij}|^2 = -2 \sum_{i,j} (\epsilon_i - \epsilon_j)^2 |(H_{\text{off-diag}})_{ij}|^2, \quad (26)$$

which formally corresponds to Eq. (25) with $\rho \rightarrow H_{\text{off-diag}}$ and $X \rightarrow H_T$. We conclude that the Wegner flow (12) generated by $\eta = [H_T, H]$,

$$\frac{dH}{dl} = [[H_T, H], H], \quad (27)$$

which is unitary, suppresses the off-diagonal part of the Hamiltonian as if it was undergoing a dephasing evolution under the action of the diagonal part.

4.2 Wegner and Toda flows

As already advanced, there are several choices of the generator η for diagonalizing a given $N \times N$ matrix $H(0)$. As a possible form, consider

$$\eta_{nm}(l) = H_{nm}(l) \operatorname{sgn}(m - n), \quad (28)$$

for $m \neq n$ and $\eta_{nn} = 0$. Equation (12) then reduces to

$$\frac{dH_{nm}(l)}{dl} = \sum_k H_{nk}(l) H_{km}(l) [\operatorname{sgn}(k - n) - \operatorname{sgn}(m - k)]. \quad (29)$$

Further, assume that the matrix $H(l)$ takes a symmetric tridiagonal form. Then, the equations for diagonal and off-diagonal components are written respectively as

$$\frac{dH_{nn}(l)}{dl} = 2(H_{n,n+1}^2(l) - H_{n-1,n}^2(l)) \quad (n = 1, 2, \dots, N), \quad (30)$$

$$\frac{dH_{n,n+1}(l)}{dl} = H_{n,n+1}(l)(H_{n+1,n+1}(l) - H_{nn}(l)) \quad (n = 1, 2, \dots, N-1), \quad (31)$$

with $H_{01} = H_{N,N+1} = 0$. This set of equations takes a closed form and is known as the Toda equations in classical nonlinear integrable systems [79–81]. We thus refer to the Hamiltonian flow generated by (28) as the Toda flow.

We note that Eq. (23) is not satisfied in the present choice of η . However, it is still guaranteed that the matrix is diagonalized at large l due to the relation

$$\frac{d}{dl} \sum_{n=1}^k H_{nn}(l) = 2H_{k,k+1}^2(l) \geq 0, \quad (32)$$

where $k = 1, 2, \dots, N$ [82, 83]. The relation for $k = 1$ denotes that $H_{11}(l)$ is a non-decreasing function. Since $\operatorname{Tr} H^2(l)$ is independent of l , each component of $H(l)$ is not divergent, if each component of the original matrix H_0 takes a finite value. We conclude that $\lim_{l \rightarrow \infty} H_{11}(l)$ converges to a finite value and $\lim_{l \rightarrow \infty} H_{12}(l) = 0$. Then, we examine the relation for $k = 2$ to conclude that $\lim_{l \rightarrow \infty} H_{22}(l)$ takes a finite value and $\lim_{l \rightarrow \infty} H_{23}(l) = 0$. We can repeat the same consideration for the other values of k to conclude that $H(l)$ is diagonalized at $l \rightarrow \infty$ keeping the eigenvalues of the matrix unchanged.

A possible realization of the tridiagonal matrix is the one-dimensional XY model with isotropic interaction [84],

$$H(l) = \frac{1}{2} \sum_{n=1}^{N-1} v_n(l) (X_n X_{n+1} + Y_n Y_{n+1}) + \frac{1}{2} \sum_{n=1}^N h_n(l) Z_n. \quad (33)$$

In the z -basis, the second term represents the diagonal part and the first term represents the off-diagonal part. The corresponding generator of the time evolution is

$$\eta(l) = \frac{i}{2} \sum_{n=1}^{N-1} v_n(l) (X_n Y_{n+1} - Y_n X_{n+1}), \quad (34)$$

and the set of coupling functions $\{v_1(l), v_2(l), \dots, v_N(l), h_1(l), h_2(l), \dots, h_{N-1}(l)\}$ satisfies the Toda equations

$$\frac{dh_n(l)}{dl} = 2(v_n^2(l) - v_{n-1}^2(l)), \quad (35)$$

$$\frac{dv_n(l)}{dl} = v_n(l)(h_{n+1}(l) - h_n(l)). \quad (36)$$

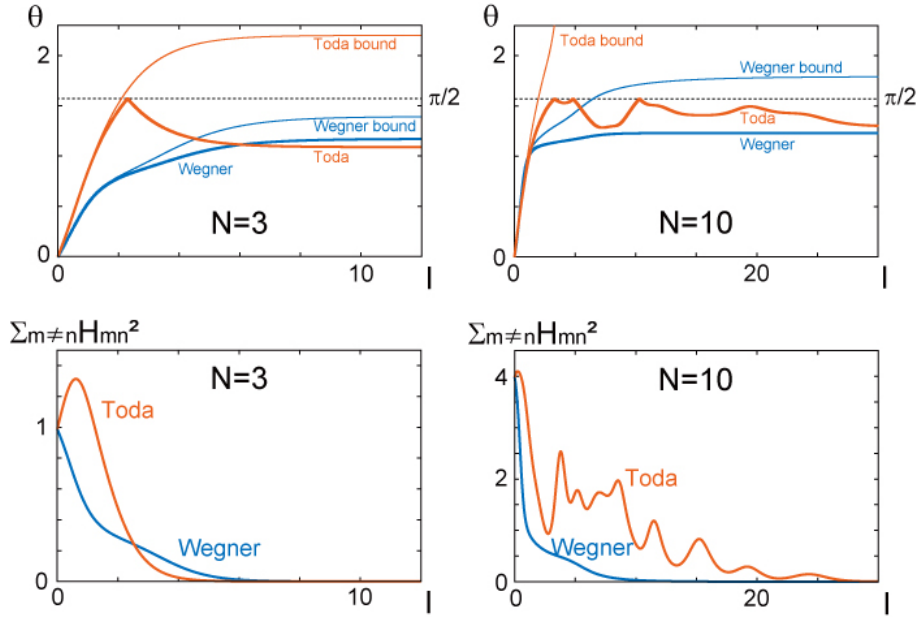


Figure 3: OQSLs for the Wegner and Toda flows. The upper panels represent $\theta(l) = \arccos\left(\text{Tr}(H(0)H(l))/\|H(0)\|^2\right)$ (bold lines) and its bound $\int_0^l ds \|\eta(s), H(s)\|/\|H\|$ (thin lines) for Wegner and Toda flows with $N = 3$ (left panel) and $N = 10$ (right). We set the initial matrix as a symmetric tridiagonal form and each component is taken from a uniform random number between -1 and 1 . In the lower panels, we plot the sum of off-diagonal components $\sum_{m \neq n} H_{mn}^2(l)$.

This Hamiltonian commutes with the total magnetization $M = \sum_{n=1}^N Z_n$ and the matrix form of the single flip sector with $M = \pm(N - 2)$ takes a tridiagonal form.

We plot examples of the Wegner and Toda flows in Fig. 3. We take a traceless symmetric tridiagonal matrix as an initial given Hamiltonian $H(0)$ in which each nonzero component is taken from a uniform random number between -1 and 1 . The numerical results in Fig. 3 implies that the Toda flow gives a tight bound for a small l and becomes worse for a large l due to the nonmonotonic decay of the off-diagonal components.

In Fig. 4, we show how the result is dependent on the dimension of the matrix N . For the Wegner flow, when N is not considerably large, the angle $\theta(l)$ between $H(0)$ and $H(l)$ grows faster by the l -evolution as N becomes large. In the Wegner flow, even though we start the time evolution from a tridiagonal form, the matrix breaks the band structure during the flow, which makes θ a large value. It does not necessarily give the property that the overlap $(H(0)|H(l))$ decays rapidly as a function of N , as we can see in some many-body systems exhibiting the orthogonality catastrophe. On the other hand, the Toda flow does not show any growing behavior as a function of N . This is due to the property that the tridiagonal form is kept throughout the time evolution. As for l_{QSL} , a saturating behavior is seen for the Wegner flow and is not seen for the Toda flow.

The independence of the Toda flow on the matrix dimension implies that we can find a tight OQSL for specific initial Hamiltonians. As we have discussed in section 3.1, saturation is possible when the flowing operator has support in only two of the eigenspaces of the generator. In what follows, we will consider the condition that the eigenvectors of the generator $\eta(l)$ are l -independent.

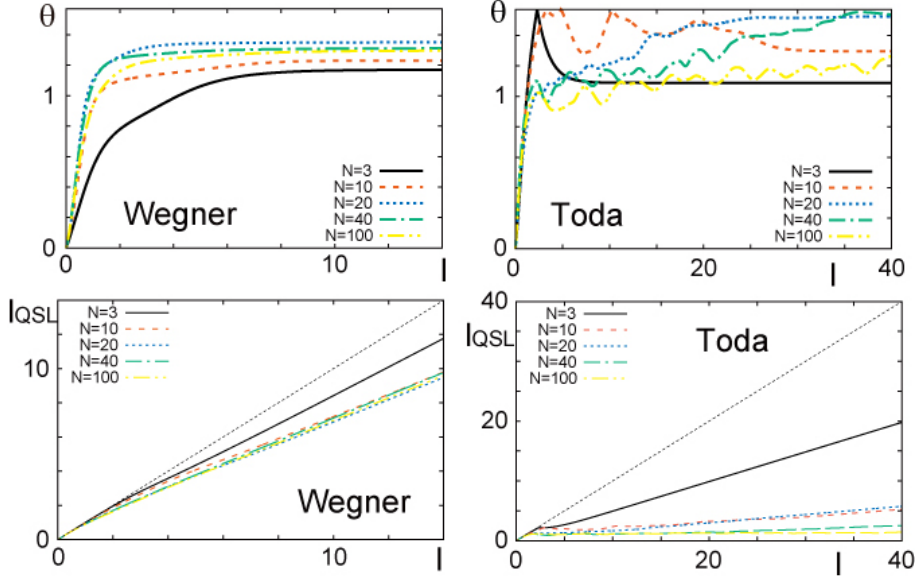


Figure 4: Plot of the $\theta(l) = \arccos\left(\text{Tr}(H(0)H(l))/\|H(0)\|^2\right)$ (top panels) and l_{QSL} (bottom panels) for several values of N . We set the initial matrix as a symmetric tridiagonal form and each component is taken from a uniform random number between -1 and 1 . The left panels represent the Wegner flow, while the right panels correspond to the Toda flow.

Hereafter, we write $H_{nn}(l) = h_n(l)$ and $H_{n,n+1}(l) = v_n(l)$. The eigenvalue equation $\eta(l)|\varphi\rangle = i\lambda(l)|\varphi\rangle$, with a real eigenvalue $\lambda(l)$ and the corresponding eigenvector $|\varphi\rangle$ is written as

$$\begin{pmatrix} \varphi_2 & 0 & & & \\ -\varphi_1 & \varphi_3 & 0 & & \\ 0 & -\varphi_2 & \varphi_4 & & \\ & \ddots & \ddots & & \\ 0 & -\varphi_{N-2} & \varphi_N & & \end{pmatrix} \begin{pmatrix} v_1(l) \\ v_2(l) \\ v_3(l) \\ \vdots \\ v_{N-1}(l) \end{pmatrix} = i\lambda(l) \begin{pmatrix} \varphi_1 \\ \varphi_2 \\ \varphi_3 \\ \vdots \\ \varphi_{N-1} \end{pmatrix}, \quad (37)$$

and $-v_{N-1}(l)\varphi_{N-1} = i\lambda(l)\varphi_N$, where $(\varphi_1, \varphi_2, \dots, \varphi_N)$ denotes the l -independent eigenvector $|\varphi\rangle$. When the diagonal components of the matrix on the left-hand side are nonzero, the matrix is invertible and $v_n(l)$ for any index n is proportional to the same l -dependent function $\lambda(l)$. The possibility that some of the components of $|\varphi\rangle$ are identically zero is excluded since that condition only results in $|\varphi\rangle = 0$.

As an exceptional case, we can find the eigenvector with $\lambda(l) = 0$ when N is odd. In that case, the eigenvector is written as

$$|\varphi\rangle \propto \left(1, 0, \frac{v_1(l)}{v_2(l)}, 0, \frac{v_3(l)v_1(l)}{v_4(l)v_2(l)}, 0, \dots, 0, \frac{v_{N-2}(l)v_{N-4}(l)\dots v_1(l)}{v_{N-1}(l)v_{N-3}(l)\dots v_2(l)}\right)^T. \quad (38)$$

The l -independence of $|\varphi\rangle$ gives the conditions $v_{2k}(l) \propto v_{2k-1}(l)$ with $k = 1, 2, \dots, (N-1)/2$.

We note that the eigenvector with $\lambda(l) = 0$ is unique if it exists. Therefore, when we impose the condition that two of the eigenvectors of $\eta(l)$ are l -independent, the dependence of $\eta(l)$

on l is described by a single function $f(l)$. Each of the nonzero components is written as

$$v_n(l) = f(l)v_n. \quad (39)$$

We insert the condition (39) into Eqs. (30) and (31) to find

$$h'_n(l) = 2f^2(l)(v_n^2 - v_{n-1}^2), \quad (40)$$

$$f'(l) = f(l)(h_{n+1}(l) - h_n(l)), \quad (41)$$

where the prime symbol denotes the derivative with respect to l . The second equation (41) shows that $h_n(l)$ is a linear function in n . Since the constant shift $h_n(l) \rightarrow h_n(l) + h_0$ does not change Eqs. (30) and (31), we set $\sum_{n=1}^N h_n(l) = 0$ and obtain

$$h_n(l) = \frac{f'(l)}{f(l)} \left(n - \frac{N+1}{2} \right). \quad (42)$$

We use this form for the first equation (40). Then, $v_n^2(l)$ is a quadratic function of n and $f(l)$ obeys the differential equation

$$\left(\frac{f'(l)}{f(l)} \right)' = -2d_1 f^2(l), \quad (43)$$

where d_1 represents a constant. The corresponding form of v_n is

$$v_n^2 = \frac{1}{2}d_1 n(N-n) + d_0, \quad (44)$$

where d_0 represents a constant.

To determine d_0 , we look at the following condition, which follows from the conservation of the norm

$$\sum_{n=1}^N h_n^2(l) + 2 \sum_{n=1}^{N-1} v_n^2(l) = \text{const.} \quad (45)$$

Without losing the generality, we can put the form $f(l) = \cos \theta(l)$. Using Eqs. (43) and (45), we find as the possible solution

$$d_0 = 0, \quad (46)$$

$$\left(\frac{\theta'(l)}{\cos \theta(l)} \right)^2 = 2d_1. \quad (47)$$

The l dependence of each component is specified as $h_n(l) = h_n \sin \theta(l)$ and $v_n(l) = v_n \cos \theta(l)$. By representing d_1 with respect to h_1 , we finally obtain

$$h_n(l) = -\frac{2h_1}{N-1} \left(n - \frac{N+1}{2} \right) \sin \theta(l), \quad (48)$$

$$v_n^2(l) = \frac{n(N-n)}{(N-1)^2} h_1^2 \cos^2 \theta(l), \quad (49)$$

and

$$\frac{\theta'(l)}{\cos \theta(l)} = \frac{2h_1}{N-1}. \quad (50)$$

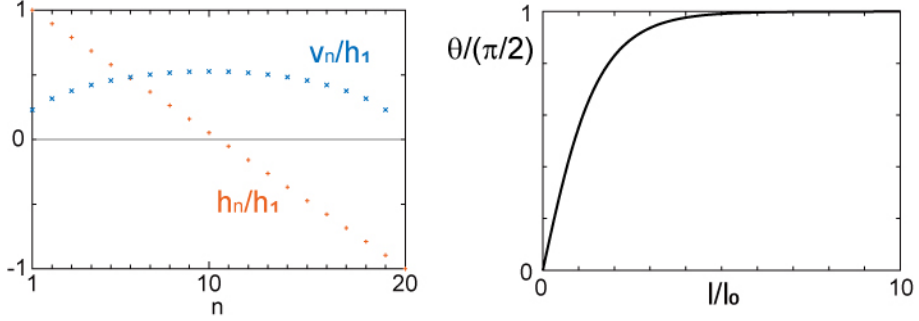


Figure 5: Left: The parameters of the initial matrix H , $\{h_n\}_{n=1,2,\dots,N}$ and $\{v_n\}_{n=1,2,\dots,N-1}$, resulting in the tight bound in the Toda flow with $N = 20$. Right: $\theta(l) = \arccos(\text{Tr}(H(0)H(l))/\|H(0)\|^2)$. We set $l_0 = (N-1)/4h_1$ and $\sin \theta(0) = 0$.

The differential equation for $\theta(l)$ is easily solved as

$$\sin \theta(l) = \frac{\sinh\left(\frac{4h_1}{N-1}l\right) + \sin \theta(0) \cosh\left(\frac{4h_1}{N-1}l\right)}{\cosh\left(\frac{4h_1}{N-1}l\right) + \sin \theta(0) \sinh\left(\frac{4h_1}{N-1}l\right)}. \quad (51)$$

In Fig. 5, we plot $\{h_n\}_{n=1,2,\dots,N}$, $\{v_n\}_{n=1,2,\dots,N-1}$, and $\theta(l)$ for $N = 20$.

All components of the matrix $H(l)$ are parameterized by a single l -dependent function $\theta(l)$, which implies that the time evolution can be denoted by a motion along an arc in the Bloch space. In fact, we find that $\theta(l)$ denotes the operator angle and the dynamics gives the tight bound:

$$\arccos \left| \frac{\text{Tr}(H(l)H(0))}{\text{Tr}(H(0)^2)} \right| = \int_0^l dt \sqrt{\frac{\text{Tr}([\eta(t), H(t)]^2)}{\text{Tr}(H(0)^2)}} = \theta(l) - \theta(0). \quad (52)$$

5 Operator Growth and Krylov Complexity

In the previous section, we have considered the flow of an observable, the Hamiltonian, with respect to a parameter different than time. Here we illustrate another application of the OQSL, pointing out that operator flows need not necessarily concern an observable. In particular, given a Liouvillian operator $\mathbb{L} = [H, \cdot]$, we show that the geometrical OQSL (7) can also be applied to the unitary flow of a superoperator, generated under the action of $\mathbb{S} = [\mathbb{L}, \cdot]$, which can be accordingly viewed as a “super Liouvillian”. This kind of flow arises naturally in characterizing the complexity of a given quantum evolution. Specifically, in the context of operator growth, the notion of Krylov complexity [54, 58–62] has recently gained attention as a measure of operator complexity for the Heisenberg evolution of an observable under the action of a time-independent Hamiltonian. The evolution of simple, local observables into increasingly complex and nonlocal ones can be described as the operator spreading in the so-called Krylov space. As mentioned in section 3.2, the latter provides the minimal subspace in which the Heisenberg dynamics unfolds and is uniquely determined by the Hamiltonian of the system and the initial operator O_0 . Krylov complexity can then be understood as the mean position of the evolving operator O_t in the so-called Krylov basis. It can be expressed as an expectation value $(O_t|\mathbb{K}O_t)$ of a corresponding (super)operator \mathbb{K} , known as the complexity operator. At this point, one can

again change representation and let the superoperators, such as \mathbb{K} , evolve while keeping the observable $|O\rangle$ fixed. We shall call this representation the super-Heisenberg picture from the evident analogy with the standard Heisenberg representation of the quantum evolution in the Hilbert space. In this picture, the complexity operator evolves accordingly to the equation

$$\dot{\mathbb{K}} = i[\mathbb{L}, \mathbb{K}] \quad (53)$$

and the corresponding unitary flow is constrained by the speed limit (7), upon identifying A and H with \mathbb{K} and \mathbb{L} , respectively. We note that our result (7) holds for finite dimensions and that the dimension of the Krylov space is always finite whenever the Hilbert space that the observables are defined over is finite [61].

5.1 Quantum dynamics in Krylov space

Let us start by briefly recalling how the Krylov space and the corresponding notion of complexity are constructed. For a more detailed discussion, we refer to [54, 58–62]. The evolution in the Heisenberg picture of an operator $O_t = e^{iHt}O_0e^{-iHt}$ can be formally written in terms of the nested commutators with the Hamiltonian H , that is, the powers of the Liouvillian $\mathbb{L} = [H, \cdot]$, as $O_t = \sum_{n=0}^{\infty} \frac{(it)^n}{n!} \mathbb{L}^n O$. The space explored during this evolution is given by the span of the infinite set $\{\mathbb{L}^n O\}_{n=0}^{\infty}$ and is precisely the Krylov space. From this infinite set, one can extract an orthonormal, finite basis $\{O_n\}_{n=0}^{D-1}$ by applying the so-called Lanczos algorithm. The first element of the basis coincides with the initial operator O_0 , which we will assume to be normalized to one. Then, at each iterative step, the next orthogonal vector is constructed as $|A_{n+1}\rangle = \mathbb{L}|O_n\rangle - b_n|O_{n-1}\rangle$, where $b_n = \|A_n\|$ is the n -th Lanczos coefficient, and the corresponding element of the Krylov basis $|O_{n+1}\rangle$ is obtained upon normalization as $O_n = A_n/b_n$. Throughout this section, we will use the Hilbert-Schmidt inner product $(A|B) = \text{Tr } A^\dagger B$ between operators. By making use of the Krylov space, the unitary evolution of the operator O_t is effectively mapped to a hopping problem on the one-dimensional, semi-infinite chain represented by the Krylov basis $\{O_n\}_{n=0}^{D-1}$, where the Lanczos coefficients b_n play the role of hopping parameters and the Liouvillian, which takes the tridiagonal form

$$\mathbb{L} = \sum_{n=0}^{D-1} b_{n+1} |O_{n+1}\rangle \langle O_n| + b_n |O_{n-1}\rangle \langle O_n|, \quad (54)$$

with $|O_{-1}\rangle = |O_D\rangle = 0$, acts as an Hamiltonian for the so-called operator wavefunction $|O_t\rangle$. The Krylov complexity operator \mathbb{K} is then defined as the position operator

$$\mathbb{K} = \sum_{n=0}^{D-1} n |O_n\rangle \langle O_n|, \quad (55)$$

on this lattice. The most studied object in this context is the expectation value of the above (super)-operator with respect to O_t and is simply known as the Krylov complexity: $K = (O_t|\mathbb{K}O_t)$. Its rate of growth is constrained by the speed limit

$$|\partial_t K(t)| \leq 2b_1 \Delta \mathbb{K}, \quad (56)$$

introduced in [62] and known as the *dispersion bound*, given that $(\Delta \mathbb{K})^2 = (O_t|\mathbb{K}^2 O_t) - (O_t|\mathbb{K} O_t)^2$ is the variance of \mathbb{K} with respect to O_t . The dispersion bound is saturated

at any time if and only if the structure of Krylov space features the so-called *complexity algebra* (57), which we shall introduce below.

It was pointed out in [59] that the Liouvillian in Krylov space, given by Eq. (54), can be written as the sum $\mathbb{L} = \mathbb{L}_+ + \mathbb{L}_-$ of raising and lowering operators that act on the Krylov basis as $\mathbb{L}_+|O_n\rangle = b_{n+1}|O_{n+1}\rangle$ and $\mathbb{L}_-|O_n\rangle = b_n|O_{n-1}\rangle$, respectively. It appears then natural to introduce a super-operator $\mathbb{B} = \mathbb{L}_+ - \mathbb{L}_-$, conjugated to the Liouvillian, and consider their commutator $\tilde{\mathbb{K}} = [\mathbb{L}, \mathbb{B}]$ [59]. The dispersion bound (56) is identically saturated if and only if these three operators close an algebra, which can only take the form [62]

$$[\mathbb{L}, \mathbb{B}] = \tilde{\mathbb{K}}, \quad [\tilde{\mathbb{K}}, \mathbb{L}] = \alpha \mathbb{B}, \quad [\tilde{\mathbb{K}}, \mathbb{B}] = \alpha \mathbb{L} \quad (57)$$

and implies also that $\tilde{\mathbb{K}} = \alpha \mathbb{K} + \gamma \mathbb{1}$, where $\alpha, \gamma \in \mathbb{R}$ [59]. The Krylov complexity growth rate is then maximal [62]. It can be shown that γ is always a positive number and α is a real number satisfying the condition $\alpha = -\frac{2\gamma}{D-1}$ for finite Krylov dimension D and $\alpha \geq 0$ if $D = \infty$ [62]. Moreover, the algebraic closure (57), or equivalently the saturation of the bound (56), implies that the Lanczos coefficients evolve according to [59, 62]

$$b_n = \sqrt{\frac{1}{4}\alpha n(n-1) + \frac{1}{2}\gamma n}. \quad (58)$$

For $\alpha > 0$, this dependence captures the asymptotic linear growth $b_n = \sqrt{\alpha}n$ conjectured by Parker *et al.* to hold in generic non-integrable systems, leading to the maximal growth of Krylov complexity [54]. A paradigmatic example of this class of systems is the celebrated Sachdev-Ye-Kitaev (SYK) model [85].

5.2 Saturation of the OQSL by the complexity algebras

In the “super” Heisenberg picture, the observable operator is kept fixed while the complexity operator \mathbb{K} evolves unitarily according to

$$\mathbb{K}_t = e^{-i\mathbb{L}t} \mathbb{K}_0 e^{i\mathbb{L}t} = \sum_{n=0}^{\infty} \frac{(-i)^n}{n!} \mathbb{S}^n(\mathbb{K}_0) t^n, \quad (59)$$

where $\mathbb{S} = [\mathbb{L}, \cdot]$ will be referred to as super Liouvillian. In the case of closed complexity algebras, thanks to the commutation relations (57), all the powers $\mathbb{S}^n(\mathbb{K}_0)$ reduce to terms proportional to either \mathbb{K}_0 or \mathbb{B} . In particular, if $\alpha \neq 0$ one can show that [62]

$$\mathbb{S}^{2n}(\mathbb{K}_0) = (-1)^n \alpha^{n-1} (\alpha \mathbb{K}_0 + \gamma \mathbb{1}), \quad (60)$$

$$\mathbb{S}^{2n+1}(\mathbb{K}_0) = (-1)^{n+1} \alpha^n \mathbb{B}, \quad (61)$$

where the first equation clearly holds only for $n > 0$, being $\mathbb{S}^0(\mathbb{K}_0) = \mathbb{K}_0$. Conversely, when $\alpha = 0$ only $\mathbb{S}(\mathbb{K}_0) = -\mathbb{B}$ and $\mathbb{S}^2(\mathbb{K}_0) = -\gamma \mathbb{1}$ survive, being $\mathbb{S}^n(\mathbb{K}_0) = 0$ for $n > 2$. Thus,

$$\mathbb{K}_t = \begin{cases} (1 - \alpha) \mathbb{K}_0 - \gamma \mathbb{1} + \cosh(\sqrt{\alpha}t) (\mathbb{K}_0 + \frac{\gamma}{\alpha} \mathbb{1}) + i \sinh(\sqrt{\alpha}t) \frac{1}{\alpha} \mathbb{B} & \alpha \neq 0, \\ \mathbb{K}_0 + i \mathbb{B}t + \frac{\gamma}{2} t^2 \mathbb{1} & \alpha = 0. \end{cases} \quad (62)$$

Equation (59), together with Eqs. (60)-(61), implies that whenever the dispersion bound (56) is saturated, the full time-evolution of the Krylov complexity operator \mathbb{K}_t must be

contained in a 3-dimensional space, spanned by the identity $\mathbb{1}$, the initial complexity \mathbb{K}_0 and $\mathbb{B} = [\mathbb{K}_0, \mathbb{L}]$:

$$\mathbb{K}_t \in \text{Span}\{\mathbb{1}, \mathbb{K}_0, \mathbb{B}\}. \quad (63)$$

This space defines the “super” Krylov space of Krylov complexity itself and turns out to be dramatically simplified by the assumption of closed complexity algebra. From the discussion in section 3.2, we can conclude that \mathbb{K}_t having a 3-dimensional Krylov space is a sufficient condition for it to saturate the refined OQSL (10). We recall that here A_t and \mathbb{L} are replaced by \mathbb{K}_t and \mathbb{S} , respectively. Then Eq. (63) implies that \mathbb{K} has support in only three eigenspaces of \mathbb{S} , one of them corresponding to the eigenvalue 0: $\mathbb{K}_t = \mathbb{P}_0 + \mathbb{P}_\omega + \mathbb{P}_{-\omega}$. Therefore, we conclude that the super operator $\mathbb{K}_t - \mathbb{P}_0$ saturates the OQSL (10); that is, it evolves along a geodesic trajectory. In other words, the maximal growth rate of Krylov complexity, leading to the saturation of the dispersion bound (56), is equivalent to the geodesic evolution of the Krylov complexity operator, provided that we subtract its stationary component \mathbb{P}_0 . Indeed, we remark that \mathbb{P}_0 is necessarily different from zero since $\text{Tr } \mathbb{K} \neq 0$, and must be removed to obtain a tight OQSL. From the explicit computation performed below, we shall conclude that the identity is indeed the only stationary component of the Krylov complexity, i.e., $\mathbb{P}_0 = \text{Tr } \mathbb{K} \frac{\mathbb{1}}{\|\mathbb{1}\|^2}$. By doing so, we shall also explicitly assess the improvement achieved by replacing the OQSL (7) with its refined counterpart (10).

5.3 Computation of the OQSL for the complexity algebras

The geometrical OQSL (7) for the Krylov complexity reads as

$$t \geq \|\mathbb{K}_0\| \frac{\arccos\left(\frac{(\mathbb{K}_0|\mathbb{K}_t)}{\|\mathbb{K}_0\|^2}\right)}{\|[\mathbb{L}, \mathbb{K}_0]\|}, \quad (64)$$

where, given a time-independent Liouvillian \mathbb{L} , the velocity of the flow $\|[\mathbb{L}, \mathbb{K}_0]\|$ is constant. The initial complexity \mathbb{K}_0 coincides with the usual Krylov complexity operator (55) in the standard Heisenberg picture. In order to assess its deviation from saturation, we explicitly evaluate the OQSL (64) in the case of the $SU(2)$ complexity algebra, that is, when the complexity growth saturates the dispersion bound (56) in finite dimension [62]. Let us define $\mathcal{V}_{\mathbb{K}} \equiv \|\mathbb{K}_0\|^{-1} \|[\mathbb{L}, \mathbb{K}_0]\|$ as the (normalized) velocity of the complexity flow. By explicit computation in the Krylov basis, one can verify that $\mathcal{V}_{\mathbb{K}}$, being $[\mathbb{L}, \mathbb{K}_0] = -\mathbb{B}$ by construction, always reduces to

$$\mathcal{V}_{\mathbb{K}}^2 = \frac{\|\mathbb{B}\|^2}{\|\mathbb{K}_0\|^2} = \frac{2}{\|\mathbb{K}_0\|^2} \sum_{n=1}^{D-1} b_n^2, \quad (65)$$

where the norm of the complexity is fixed by the Krylov dimension as

$$\|\mathbb{K}_0\|^2 = \sum_{n=0}^{D-1} n^2 = \frac{D(D-1)(2D-1)}{6}. \quad (66)$$

The velocity (65) of the complexity flow is maximized whenever the Lanczos coefficients growth is maximal, i.e., linear in n , which is the case for maximally chaotic systems according to the universal growth hypothesis [54]. Indeed, by focusing on the initial scrambling period and neglecting the role of the following plateau and descent in the b_n ’s [61], we

conclude that a sub-polynomial behavior $b_n \propto n^\delta$ with $0 < \delta < 1$ always leads to a smaller velocity $\mathcal{V}_{\mathbb{K}}$ than the linear growth $b_n \propto n$. We stress that this observation also holds for infinite-dimensional Krylov spaces. As shown below, the velocity (65) remains finite in this limit, and once we fix the proportionality constant, the velocity is maximized by the linear growth of the b_n 's. In other words, according to the universal growth hypothesis [54], complexity flows at the highest speed in maximally chaotic systems.

Let us now focus on the instances of Krylov dynamics that saturate another notion of the speed limit for operator growth, namely the above-mentioned dispersion bound (56). As reviewed above, in such cases, the dynamics of Krylov complexity is determined by an underlying 3-dimensional algebra [62] and the Lanczos coefficients obey Eq. (58). As a result, the velocity (65) of the complexity flow can be expressed as

$$\mathcal{V}_{\mathbb{K}}^2 = \frac{\alpha(D-2) + 3\gamma}{2D-1}. \quad (67)$$

Before restricting the analysis to the finite-dimensional case $\alpha < 0$, where the geometrical QSL (7) can be applied, let us stress that this notion of velocity is well defined also in the limit $D \rightarrow \infty$, where $\alpha \geq 0$. In particular, if $\alpha > 0$, when the Krylov complexity diverges exponentially with time as $K(t) \sim e^{\sqrt{\alpha}t}$ [59, 62], we obtain that $\mathcal{V}_{\mathbb{K}} \rightarrow \sqrt{\alpha/2}$: the speed of the complexity operator flow is proportional to the characteristic time scale of the exponential divergence of the Krylov complexity. Instead, if $\alpha = 0$, which leads to a quadratic divergence of K [59, 62], the above-defined speed of the flow vanishes. This singular behavior can be understood as the QSL (64), derived under the assumption of finite dimension D , may not have a well-defined counterpart for $D \rightarrow \infty$. In particular, as we shall see below, the numerator in Eq. (64) also vanishes for $\alpha = 0$, resulting in an indeterminate form 0/0. Finally, for the Krylov dynamics to saturate the dispersion bound (56) over a finite-dimensional space, the underlying complexity algebra must be that of $SU(2)$, corresponding to the case $\alpha < 0$ [62]. In such case, given the condition $b_D = 0$, the parameters α and γ of Eq. (58) are subject to the further constraint $2\gamma = |\alpha|(D-1)$ [62], which also ensures the expression (67) to be positive. Indeed, the velocity of the complexity flow generated by the $SU(2)$ algebra reduces to $\mathcal{V}_{\mathbb{K}}^2 = |\alpha|(D+1)/[2(2D-1)]$. For this class of models, we compute the QSL (64) exactly, thus establishing a direct comparison between the geometrical OQSL introduced in the present work and the dispersion bound that constraints the growth of Krylov complexity [62].

In addition to the velocity of the flow, the other quantity that characterizes the speed limit is the notion of distance spanned during the evolution, which appears at the numerator of Eqs. (7) and (64) and is given in terms of the autocorrelation function, i.e., the operator overlap. In the case of closed complexity algebras, the autocorrelation function of the complexity

$$(\mathbb{K}_0|\mathbb{K}_t) = \sum_{n=0}^{\infty} \frac{(-i)^n}{n!} (\mathbb{K}_0|\mathbb{S}^n(\mathbb{K}_0)) t^n \quad (68)$$

can be explicitly evaluated by making use of Eqs. (60)-(61). We note that, since $(\mathbb{K}_0|\mathbb{B}) = 0$, only the even powers of the super Liouvillian \mathbb{S} contribute to the sum in Eq. (68). Moreover, the only finite-dimensional case where we can straightforwardly apply the OQSL (64) is that of the $SU(2)$ complexity algebra, i.e., when $\alpha < 0$. For this class of models, by substituting Eqs. (60)-(61) into the expression (68) and recognizing the Taylor expansion

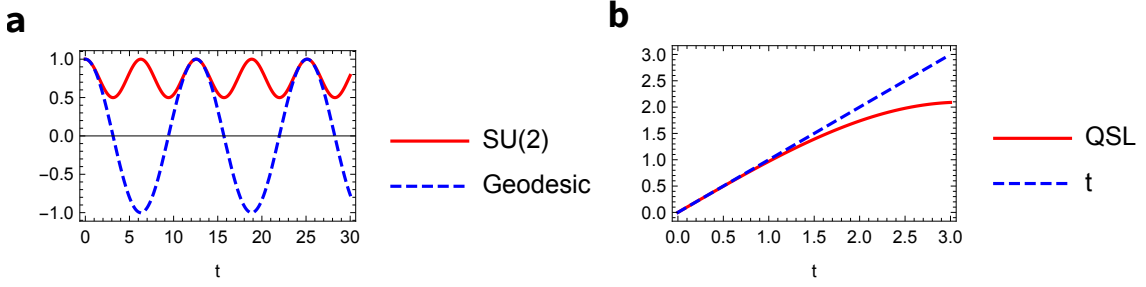


Figure 6: We illustrate the deviation from the saturation of the OQSL (64) for the $SU(2)$ complexity algebra, with Krylov dimension $D = 1000$ and $\alpha = -1$. **a** We compare the evolution (69) of the complexity autocorrelation function $(\mathbb{K}_0|\mathbb{K}_t)$ (red curve) with the geodesic trajectory $(\mathbb{K}_0|\mathbb{K}_t)|_{\text{geodesic}}$ (71) (blue dashed curve). **b** We show the left and right-hand side of the inequality (70) (blue dashed and red curves, respectively). The OQSL is tight only near $t = 0$, and the deviation increases with time.

of the cosine, we obtain

$$(\mathbb{K}_0|\mathbb{K}_t) = (\|\mathbb{K}\|^2 + \frac{\gamma}{\alpha} \text{Tr } \mathbb{K}) \cos \sqrt{|\alpha|}t - \frac{\gamma}{\alpha} \text{Tr } \mathbb{K}, \quad (69)$$

where $\text{Tr } \mathbb{K} = D(D-1)/2$ and $\|\mathbb{K}\|^2$ is given by Eq. (66). Therefore, in the case of the $SU(2)$ complexity algebra, the autocorrelation function $(\mathbb{K}_0|\mathbb{K}_t)$ oscillates at the frequency $\sqrt{|\alpha|}$, which, we note, is half the frequency of oscillation of the Krylov complexity K itself [62]. By substituting Eq. (69) into Eq. (64) and using that $2\gamma = |\alpha|(D-1)$, we rewrite the OQSL as

$$t \geq \frac{1}{\mathcal{V}_{\mathbb{K}}} \arccos \left[\left(1 - \frac{3(D-1)}{2(2D-1)} \right) \cos \sqrt{|\alpha|}t + \frac{3(D-1)}{2(2D-1)} \right], \quad (70)$$

where $\mathcal{V}_{\mathbb{K}}^2 = |\alpha|(D+1)/[2(2D-1)]$. As argued above, we expect this bound not to be tight due to the presence of a stationary component in the complexity flow given by the non-vanishing of its trace. We illustrate the deviation from the geodesic trajectory

$$(\mathbb{K}_0|\mathbb{K}_t)|_{\text{geodesic}} = \|\mathbb{K}\|^2 \cos \mathcal{V}_{\mathbb{K}} t \quad (71)$$

and the divergence of the two sides of Eq. (70) in Fig. 6. In what follows, we shall explicitly remove the stationary component of the complexity flow, thus proving the saturation of the refined OQSL (10) and showing its equivalence with the dispersion bound (56).

Finally, although the framework of the geometrical QSL requires a finite dimension, it is instructive to consider the behavior of the quantities involved in Eq. (64) as $D \rightarrow \infty$. In particular, we have already stressed above that the velocity $\mathcal{V}_{\mathbb{K}}$ (65) of the complexity flow remains finite, is non-zero for $\alpha > 0$ and vanishes for $\alpha = 0$. Moreover, from Eq. (68), with analogous steps as for the $SU(2)$, we obtain that for $\alpha = 0$ the autocorrelation function behaves as $(\mathbb{K}_0|\mathbb{K}_t) = \|\mathbb{K}\|^2 + \frac{\gamma}{2}t^2$. At any finite time, this implies the vanishing of the numerator of the QSL (64), since the argument of the arccosine approaches 1 as $D \rightarrow \infty$. The evaluation of the limit of the full expression yields as a result that $\tau_{\text{QSL}} \rightarrow 0$ as $D \rightarrow \infty$ in the case of the HW algebra, i.e., for $\alpha = 0$. Conversely, the notion of distance employed in our QSL (7) is not well defined in the case $\alpha > 0$, since the normalized autocorrelation function diverges exponentially with time, $(\mathbb{K}_0|\mathbb{K}_t)/\|\mathbb{K}\|^2 \sim \exp\{\sqrt{\alpha}t\}$.

5.3.1 Saturation of the refined OQSL

The fact that the Krylov complexity operator \mathbb{K}_t cannot saturate the OQSL (64) is already evident from the observation that $\text{Tr } \mathbb{K}_t \neq 0$, as this condition results in a non-zero stationary component \mathbb{P}_0 . In particular, the trace accounts for the stationary component along the identity. Removing the trace is sufficient to achieve saturation only if there are no other stationary components of \mathbb{K}_t , meaning that the zero eigenvalue of the super Liouvillian \mathbb{S} has no degeneracy, such that the corresponding eigenspace is spanned by the identity. We explicitly show that this is indeed the case for closed complexity algebras. In this sense, the dispersion bound (56) and the OQSL (10) provide a unique constraint on the operator growth in Krylov space and the saturation of the former automatically implies the saturation of the latter.

Let us, therefore, consider the operator $\bar{\mathbb{K}}_t$ obtained by subtracting from the Krylov complexity its component along the identity:

$$\bar{\mathbb{K}}_t = \mathbb{K}_t - (\mathbb{K}_t | \mathbb{1}) \frac{\mathbb{1}}{\|\mathbb{1}\|^2}, \quad (72)$$

where $(\mathbb{K}_t | \mathbb{1}) = \text{Tr } \mathbb{K}$ and $\|\mathbb{1}\|^2 = D$. The OQSL (7) for $\bar{\mathbb{K}}_t$ reads as

$$t \geq \frac{\arccos\left(\frac{(\bar{\mathbb{K}}_0 | \bar{\mathbb{K}}_t)}{\|\bar{\mathbb{K}}\|^2}\right)}{\mathcal{V}_{\bar{\mathbb{K}}}}, \quad (73)$$

where $\mathcal{V}_{\bar{\mathbb{K}}}^2 = \|\mathbb{B}\|^2 / \|\bar{\mathbb{K}}\|^2$. Now, by using Eq. (66) and that $\text{Tr } \mathbb{K} = D(D-1)/2$, we obtain

$$\|\bar{\mathbb{K}}\|^2 = \|\mathbb{K}\|^2 - \frac{(\text{Tr } \mathbb{K})^2}{D} = \frac{D(D^2-1)}{12}. \quad (74)$$

Moreover, in the case of $SU(2)$ complexity algebra, from Eq. (58) with $\alpha < 0$ and $2\gamma = |\alpha|(D-1)$ we find

$$\|\mathbb{B}\|^2 = 2 \sum_{n=1}^{D-1} b_n^2 = |\alpha| \frac{D(D^2-1)}{12}. \quad (75)$$

By taking the ratio of the expressions above, we conclude that the velocity of the $\bar{\mathbb{K}}_t$ flow for the $SU(2)$ complexity algebra is $\mathcal{V}_{\bar{\mathbb{K}}} = \sqrt{|\alpha|}$. On the other hand, the autocorrelation function $(\bar{\mathbb{K}}_0 | \bar{\mathbb{K}}_t)$ can be computed analogously to the one of \mathbb{K}_t in Eqs. (68)-(69), with the only difference that now $\text{Tr } \bar{\mathbb{K}} = 0$. We thus obtain

$$(\bar{\mathbb{K}}_0 | \bar{\mathbb{K}}_t) = \|\bar{\mathbb{K}}\|^2 \cos \sqrt{|\alpha|} t = \|\bar{\mathbb{K}}\|^2 \cos \mathcal{V}_{\bar{\mathbb{K}}} t, \quad (76)$$

which implies that the inequality in the OQSL (73) reduces to an identity at any time. In conclusion, the saturation of the dispersion bound (56) in finite dimension implies that the Krylov complexity \mathbb{K}_t also saturates the refined OQSL (10) with $\mathbb{P}_0 = \mathbb{1} \text{Tr } \mathbb{K}/D$. We illustrate this saturation in Fig. (7). From the comparison between Figs. 6 and (7) we can assess the efficiency of the refined OQSL (10) in yielding a tight evolution by removing the components that do not contribute dynamically to the flow.

6 Conclusions, Discussion and Outlook

Conventional QSLs bound the minimum time for the completion of a process by quantifying the distance traveled by the system along the evolution in state space. OQSLs generalize

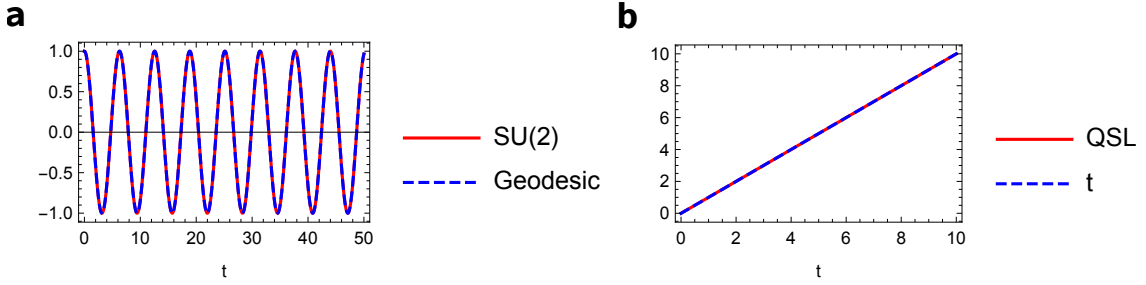


Figure 7: Illustration of the saturation of the OQSL (73) for the $SU(2)$ complexity algebra, with Krylov dimension $D = 1000$ and $\alpha = -1$. **a** The complexity autocorrelation function ($\bar{K}_0|\bar{K}_t$) (76) (red curve) is shown to match the geodesic trajectory (blue dashed curve). **b** The left-hand and right-hand sides of the inequality (73) (blue dashed and red curves, respectively). The OQSL reduces to an identity at any time.

the scope of conventional QSL to account for processes described in terms of operator flows, i.e., the change of an operator resulting from a conjugation by a one-parameter unitary [56]. In this work, we have introduced a geometric OQSL that holds for arbitrary unitaries, i.e., whether the generator of flow is parameter dependent or not. In addition, we have shown the bound to be tight and identified the required conditions for its saturation. This has led us to introduce a refined OQSL upon identifying the subspace in which the dynamics unfolds.

The usefulness of these OQSLs has been illustrated in the context of a continuous renormalization group formulated as a Wegner Hamiltonian flow for block diagonalization. In this context, we have shown that Wegner’s choice of the flow generator leads to a monotonic decay of the off-diagonal elements of the flowing Hamiltonian towards the target block-diagonal one. However, such a choice does not saturate the OQSL. By contrast, an alternative choice of the generator associated with the Toda flow can lead to the saturation of the OQSL for a specific family of initial Hamiltonians. Beyond the case of Wegner Hamiltonian flows, we expect our results to apply to other schemes for Hamiltonian diagonalization, such as those relying on the Schrieffer-Wolff transformation [86].

We have further discussed the implication of our results in the context of operator growth in Krylov space. In this representation, the time evolution of an operator is analogous to the spreading of a particle in the Krylov lattice, where the mean position is a proxy for operator complexity. The conditions for maximal operator growth are then associated with the saturation of the dispersion bound [62], which occurs when the Lanczos coefficients exhibit a specific dependence on the lattice site index. Here, we have introduced a “super-Heisenberg” representation of the Krylov complexity operator generated by a super Liouvillian. Making use of the OQSL in such representation, we have shown that the saturation of the dispersion bound implies the saturation of the OQSL for the Krylov complexity operator. The application of OQSL to other complexity measures, such as the family of q -complexities including out-of-time-order correlators [54], offers an interesting prospect.

Beyond these examples, we expect OQSLs to find manifold applications in the characterization of nonequilibrium phenomena, such as the crossing of a quantum phase transition, the equilibration and thermalization of isolated many-body systems, quantum thermody-

namic processes, quantum control, and quantum annealing. In addition, OQSL may be used in the study of integrable systems, using the zero-curvature representation [87], Lax pairs [88], and Hamiltonian deformations [89–91]. The generalization of our results to dissipative quantum systems would be highly desirable, given its prospective applications, e.g., to the description of open quantum dynamics in Heisenberg’s representation and the quest for fundamental limits to nonunitary operator growth [92, 93].

7 Acknowledgements

It is a pleasure to acknowledge discussions with Léonce Dupays, Íñigo L. Egusquiza and Federico Roccati. KT acknowledges support by JSPS KAKENHI grant No. JP20K03781 and No. JP20H01827.

Appendices

A Proving bijection between positive semi-definite inner-products and positive semi-definite operators

Lemma 1. *Let $\mathcal{P} \in \text{End}(\mathcal{B})$ be a positive semi-definite superoperator. The binary operation $\langle \cdot, \mathcal{P} \cdot \rangle_H : \mathcal{B} \times \mathcal{B} \rightarrow \mathbb{R}$ is a positive semi-definite inner product on \mathcal{B} .*

Proof. We need to show that the map $\langle \cdot, \mathcal{P} \cdot \rangle_H$ satisfies linearity, Hermitian symmetry, and positive semi-definiteness.

Linearity

Consider any triplet of operators A , B and C and a complex number λ . We then have

$$\langle A, \mathcal{P} \lambda B \rangle_H = \langle A, \lambda \mathcal{P} B \rangle_H = \lambda \langle A, \mathcal{P} B \rangle_H \quad (77)$$

$$\langle A, \mathcal{P}(B + C) \rangle_H = \langle A, \mathcal{P}B + \mathcal{P}C \rangle_H = \langle A, \mathcal{P}B \rangle_H + \langle A, \mathcal{P}C \rangle_H, \quad (78)$$

where we have used the linearity of the Hilbert-Schmidt inner product and the superoperator.

Hermitian symmetry

For any pair of operators A and B we have

$$\langle A, \mathcal{P}B \rangle_H = \langle \mathcal{P}B, A \rangle_H^* = \langle B, \mathcal{P}^\dagger(A) \rangle_H^* = \langle B, \mathcal{P}A \rangle_H^*, \quad (79)$$

where we have used the Hermitian symmetry property of the Hilbert-Schmidt inner product and the fact that a positive semi-definite superoperator is self-adjoint.

Positive semi-definiteness

From the definition of positive semi-definiteness of a superoperator it follows directly that

$$\langle A, \mathcal{P}A \rangle_H \geq 0, \quad (80)$$

for any operator A . ■

Proposition 2. *Given the Hilbert space $(\mathcal{B}, \langle \cdot, \cdot \rangle_H)$, the map $\mathcal{P} \mapsto \langle \cdot, \mathcal{P} \cdot \rangle_H$ is a bijection between the set of positive semi-definite operators on $(\mathcal{B}, \langle \cdot, \cdot \rangle_H)$ and the set of positive semi-definite inner products on \mathcal{B} .*

Proof. We can prove that the map is a bijection if we can prove that it is injective and surjective.

Injectivity

Suppose that $\langle \cdot, \mathcal{P} \cdot \rangle_H = \langle \cdot, \eta(\cdot) \rangle_H$ for some pair of superoperators \mathcal{P} and η . It follows that

$$\begin{aligned} \langle \cdot, \mathcal{P} \cdot \rangle_H = \langle \cdot, \eta(\cdot) \rangle_H &\iff \langle A, \mathcal{P}B \rangle_H = \langle A, \eta(B) \rangle_H \quad \forall A, B \in \mathcal{B} \\ &\iff \mathcal{P} = \eta. \end{aligned} \tag{81}$$

Surjectivity

Given any positive semi-definite inner product $(\cdot | \cdot)$, we want to construct a positive semi-definite superoperator \mathcal{P} such that $(\cdot | \cdot) = \langle \cdot, \mathcal{P} \cdot \rangle_H$. Let $M_1, M_2 \dots M_{n^2}$ be an operator basis in \mathcal{B} and a_k and b_k be the corresponding components of A and B . Define $\langle M_i, \mathcal{P} M_j \rangle_H = (M_i | M_j)$. This superoperator is positive semi-definite since

$$\begin{aligned} \langle A, \mathcal{P}B \rangle_H &= \sum_{i=1}^{n^2} \sum_{j=1}^{n^2} a_i^* b_j \langle M_i, \mathcal{P} M_j \rangle_H = \sum_{i=1}^{n^2} \sum_{j=1}^{n^2} a_i^* b_j (M_i | M_j) \\ &= (A | B) \implies \langle A, \mathcal{P}A \rangle_H = (A | A) \geq 0, \end{aligned} \tag{82}$$

from which it is also clear that \mathcal{P} maps to $(\cdot | \cdot)$. ■

B The kernel of seminorms

Proposition 3. *Let $\|\cdot\|$ be the seminorm induced by the positive semi-definite inner product $\langle \cdot, \mathcal{P} \cdot \rangle_H$. It is then the case that $\|A\| = 0 \iff \mathcal{P}A = 0$.*

Proof. Let $\{M_k\}_{k=0}^{n^2}$ be an orthonormal eigenbasis of \mathcal{P} such that λ_k is the eigenvalue corresponding to the eigenvector M_k . Let a_k be the components of an operator A . We then have

$$\begin{aligned} \langle A, \mathcal{P}A \rangle_H &= \sum_{i=1}^{n^2} \sum_{j=1}^{n^2} a_i^* a_j \langle M_i, \mathcal{P} M_j \rangle_H = \sum_{i=1}^{n^2} \sum_{j=1}^{n^2} a_i^* a_j \lambda_j \delta_{ij} \\ &= \sum_{k=1}^{n^2} |a_k|^2 \lambda_k. \end{aligned} \tag{83}$$

Since $\lambda_k \geq 0$, this sum can only be zero if $a_k = 0$ for $\lambda_k > 0$, in other words, A lies in the kernel of \mathcal{P} . ■

C Proof of equation 4

Proof. Define $\tilde{A} = A - \hat{A}$. We can choose an orthogonal basis $M_1, M_2, \dots, M_d, N_1, N_2, \dots, N_{n-d}$, such that the operators M_k and N_k span $\text{im}(\mathcal{P})$ and $\text{ker}(\mathcal{P})$ respectively and d is the dimension of $\text{im}(\mathcal{P})$. Let a_k be the components of A with respect to this basis. We have that

$$\begin{aligned} \mathcal{P}\tilde{A} &= \mathcal{P}(A - \hat{A}) = \mathcal{P}A - \mathcal{P}\hat{A} \\ &= \sum_{k=1}^d a_k \mathcal{P}M_k + \sum_{k=1}^{n-d} a_k \mathcal{P}N_k - \sum_{k=1}^d a_k \mathcal{P}M_k = 0. \end{aligned} \tag{84}$$

Using this together with linearity of $(\cdot|\cdot)$, we get

$$(A|B) = (\hat{A}|\hat{B}) + (\hat{A}|\tilde{B}) + (\tilde{A}|\hat{B}) + (\tilde{A}|\tilde{B}) = (\hat{A}|\hat{B}) = \langle \hat{A}|\hat{B} \rangle, \quad (85)$$

where the step to the second equality follows from proposition 3 and the last step follows from the definition of $\langle \cdot, \cdot \rangle$. \blacksquare

D Smallest subspace containing the dynamics

Let V be a real or complex finite dimensional vector space and let L be a linear endomorphism on V . Assuming that L is diagonalizable, we can write $L = \sum_{i=1}^d l_i P_i$, where l_i are the d distinct eigenvalues of L and P_i are the projections onto the corresponding eigenspaces satisfying $\sum_{i=1}^d P_i = I$ and $P_i P_j = \delta_{ij} P_i$. Here I is the identity map on V . It follows from the definition of the exponential function that $e^{Lt} = \sum_{i=1}^d e^{l_i t} P_i$. Consider now any initial vector v in V evolving according to $v(t) = e^{Lt}v$. Let us define the subspace $W = \text{span}\{v_i\}_{i \in I}$ where $i \in I \iff v_i := P_i v \neq 0$. We then have that $v(t) = \sum_{i \in I} e^{l_i t} v_i$ and we see that the evolution is entirely contained in W . Given a proper time interval $T \subset \mathbb{R}$, we now ask whether W is the smallest subspace for which $\{v(t) : t \in T\}$ is contained in.⁹ The answer is affirmative. To show this, first, note that the functions $e^{l_i t}$ with domain T are linearly independent given that all eigenvalues l_i are distinct. This implies that

$$\sum_{i \in I} c_i e^{l_i t} = 0 \quad \forall t \in T \iff c_i = 0 \quad \forall i \in I, \quad (86)$$

where $c_i \in \mathbb{C}$. We will use proof by contradiction to show that W must be the smallest subspace. Assume that there exists a subspace \tilde{W} containing the evolution with a dimension strictly smaller than W . We must then have the evolution contained in the subspace given by the intersection $F = W \cap \tilde{W}$. By our assumption, F must then have a dimension strictly smaller than W . This implies that there exists a non-zero linear functional w with domain W for which $F \subset \ker(w)$. We can expand this functional in the basis $\{f_i\}_{i \in I}$ defined by $f_i(v_j) = \delta_{ij}$ so that $w = \sum_{i \in I} w_i f_i$, where $w_i = w(v_i)$. We get that $w(v(t)) = 0 \quad \forall t \in T \iff \sum_{i \in I} w_i e^{l_i t} = 0 \quad \forall t \in T$. This last expression together with (86) implies that $w_i = 0 \quad \forall i \in I \iff w = 0$. Thus, we have reached a contradiction; hence, W is the smallest subspace containing $\{v(t) : t \in T\}$.

The proof can be carried out analogously for the case when L is time dependent but commutes, i.e., $[L(t_1), L(t_2)] = 0 \quad \forall t_1, t_2 \in T$.

E Optimal refinement

Consider the decomposition $\hat{A} = S + V_t$ discussed in section 2.3 and assume that the subspace $\ker(\mathbb{L}) \cap \mathcal{H}_P$ does not change over time. Suppose V_t has a non-zero projection S' onto $\ker(\mathbb{L}) \cap \mathcal{H}_P$ then S' is guaranteed to remain unchanged since we have by the assumption that $\ker(\mathbb{L}) \cap \mathcal{H}_P$ is time-independent. Let V'_t be the orthogonal complement so that $V = S' + V'_t$. It follows that

$$\langle V, V_t \rangle = (V|V_t) = (S' + V'|S' + V'_t) = (V'|V'_t) + \|S'\|^2. \quad (87)$$

⁹A proper interval is an interval in \mathbb{R} excluding the empty set and singletons.

This implies that

$$\operatorname{Re}(V'|V'_t) = \operatorname{Re}(V|V_t) - \|S'\|^2 = \operatorname{Re}C(t) - \|S\|^2 - \|S'\|^2 = \operatorname{Re}C(t) - \|S + S'\|^2, \quad (88)$$

where the last equality follows from the assumption $\operatorname{Re}\langle S, V_t \rangle = 0$. We can thus improve the speed limit further whenever $S' \neq 0$ since we would then have that $\|S + S'\| > \|S\| + \|S'\| > \|S\|$. The operator $P_0 = S + S'$ is precisely the orthogonal projection of \hat{A}_t onto $\ker(\mathbb{L}) \cap \mathcal{H}_{\mathcal{P}}$.

F Proving orthogonality from the preservation of norm

We here want to show that the operators P_0 , X_ω and Y_ω in (11) are orthogonal and that X_ω and Y_ω have the same norm. Using (11), we get that

$$\|A_t\|^2 = \|P_0\|^2 + \|P_\omega\|^2 + \|P_{-\omega}\|^2 + 2 \cos \theta(t) \operatorname{Re}\langle P_0, X_\omega \rangle + 2 \cos(2\theta(t)) \operatorname{Re}\langle P_\omega, P_{-\omega} \rangle \quad (89)$$

$$= \|P_0\|^2 + \|P_\omega\|^2 + \|P_{-\omega}\|^2 + 2 \sin \theta(t) \operatorname{Re}\langle P_0, Y_\omega \rangle + 2 \cos(2\theta(t)) \operatorname{Re}\langle P_\omega, P_{-\omega} \rangle. \quad (90)$$

At time $t = 0$, we have that $\theta(0) = 0$ and we get from expression (89) and (90) that $\operatorname{Re}\langle P_0, X_\omega \rangle = 0$. Assuming that $\theta(t)$ is not zero over the whole interval $[0, \tau]$, we can conclude from $\operatorname{Re}\langle P_0, X_\omega \rangle = 0$, (89) and (90) that $\operatorname{Re}\langle P_0, Y_\omega \rangle = 0$ must also hold. This in turn implies that $\operatorname{Re}\langle P_\omega, P_{-\omega} \rangle = 0$ since $\|A_t\|$ must be constant. This last equality guarantees that the norm of X_ω and Y_ω are equal. Note that in the case when $\theta(t) = 0$ over the whole interval, we have that the dynamics is stationary.

References

- [1] P. Pfeifer and J. Fröhlich, “Generalized time-energy uncertainty relations and bounds on lifetimes of resonances,” *Rev. Mod. Phys.* **67**, 759–779 (1995).
- [2] P. Busch, “The time–energy uncertainty relation,” in *Time in Quantum Mechanics*, edited by J. G. Muga, R. S. Mayato, and Í. L. Egusquiza (Springer Berlin Heidelberg, Berlin, Heidelberg, 2008) pp. 73–105.
- [3] L. S. Schulman, “Jump time and passage time: The duration of a quantum transition,” in *Time in Quantum Mechanics*, edited by J. G. Muga, R. Sala Mayato, and Í. L. Egusquiza (Springer Berlin Heidelberg, Berlin, Heidelberg, 2008) pp. 107–128.
- [4] V. V. Dodonov and A. V. Dodonov, “Energy–time and frequency–time uncertainty relations: exact inequalities,” *Physica Scripta* **90**, 074049 (2015).
- [5] L. Mandelstam and I. Tamm, “The uncertainty relation between energy and time in non-relativistic quantum mechanics,” in *Selected Papers*, edited by Boris M. Bologtovskii, Victor Ya. Frenkel, and Rudolf Peierls (Springer Berlin Heidelberg, Berlin, Heidelberg, 1991) pp. 115–123.
- [6] S. Deffner and S. Campbell, “Quantum speed limits: from Heisenberg’s uncertainty principle to optimal quantum control,” *Journal of Physics A: Mathematical and Theoretical* **50**, 453001 (2017).
- [7] Z. Gong and R. Hamazaki, “Bounds in nonequilibrium quantum dynamics,” *International Journal of Modern Physics B* **36**, 2230007 (2022).

[8] N. Margolus and L. B. Levitin, “The maximum speed of dynamical evolution,” *Physica D: Nonlinear Phenomena* **120**, 188–195 (1998), proceedings of the Fourth Workshop on Physics and Consumption.

[9] B. Zieliński and M. Zych, “Generalization of the margolus-levitin bound,” *Phys. Rev. A* **74**, 034301 (2006).

[10] N. Margolus, “The finite-state character of physical dynamics,” arXiv e-prints , arXiv:1109.4994 (2011), arXiv:1109.4994 [quant-ph] .

[11] A. Uhlmann, “An energy dispersion estimate,” *Physics Letters A* **161**, 329–331 (1992).

[12] S. Deffner and E. Lutz, “Energy–time uncertainty relation for driven quantum systems,” *Journal of Physics A: Mathematical and Theoretical* **46**, 335302 (2013).

[13] M. Okuyama and M. Ohzeki, “Comment on ‘energy-time uncertainty relation for driven quantum systems’,” *Journal of Physics A: Mathematical and Theoretical* **51**, 318001 (2018).

[14] M. M. Taddei, B. M. Escher, L. Davidovich, and R. L. de Matos Filho, “Quantum speed limit for physical processes,” *Phys. Rev. Lett.* **110**, 050402 (2013).

[15] A. del Campo, I. L. Egusquiza, M. B. Plenio, and S. F. Huelga, “Quantum speed limits in open system dynamics,” *Phys. Rev. Lett.* **110**, 050403 (2013).

[16] S. Deffner and E. Lutz, “Quantum speed limit for non-markovian dynamics,” *Phys. Rev. Lett.* **111**, 010402 (2013).

[17] F. Campaioli, F. A. Pollock, and K. Modi, “Tight, robust, and feasible quantum speed limits for open dynamics,” *Quantum* **3**, 168 (2019).

[18] L. P. García-Pintos and A. del Campo, “Quantum speed limits under continuous quantum measurements,” *New Journal of Physics* **21**, 033012 (2019).

[19] B. Shanahan, A. Chenu, N. Margolus, and A. del Campo, “Quantum speed limits across the quantum-to-classical transition,” *Phys. Rev. Lett.* **120**, 070401 (2018).

[20] M. Okuyama and M. Ohzeki, “Quantum speed limit is not quantum,” *Phys. Rev. Lett.* **120**, 070402 (2018).

[21] N. Shiraishi, K. Funo, and K. Saito, “Speed limit for classical stochastic processes,” *Phys. Rev. Lett.* **121**, 070601 (2018).

[22] S. B. Nicholson, L. P. García-Pintos, A. del Campo, and J. R. Green, “Time–information uncertainty relations in thermodynamics,” *Nature Physics* **16**, 1211–1215 (2020).

[23] V. T. Vo, T. Van Vu, and Y. Hasegawa, “Unified approach to classical speed limit and thermodynamic uncertainty relation,” *Phys. Rev. E* **102**, 062132 (2020).

[24] T. Van Vu and Y. Hasegawa, “Geometrical bounds of the irreversibility in markovian systems,” *Phys. Rev. Lett.* **126**, 010601 (2021).

[25] L. P. García-Pintos, S. B. Nicholson, J. R. Green, A. del Campo, and A. V. Gorshkov, “Unifying quantum and classical speed limits on observables,” *Phys. Rev. X* **12**, 011038 (2022).

[26] I. Bengtsson and K. Życzkowski, *Geometry of Quantum States: An Introduction to Quantum Entanglement*, 2nd ed. (Cambridge University Press, 2017).

[27] D. P. Pires, M. Cianciaruso, L. C. Céleri, G. Adesso, and D. O. Soares-Pinto, “Generalized geometric quantum speed limits,” *Phys. Rev. X* **6**, 021031 (2016).

[28] F. Campaioli, F. A. Pollock, F. C. Binder, and K. Modi, “Tightening quantum speed limits for almost all states,” *Phys. Rev. Lett.* **120**, 060409 (2018).

[29] N. Hörnedal, D. Allan, and O. Sönnernborn, “Extensions of the mandelstam–tamm quantum speed limit to systems in mixed states,” *New Journal of Physics* **24**, 055004 (2022).

[30] M. Bukov, D. Sels, and A. Polkovnikov, “Geometric speed limit of accessible many-body state preparation,” *Phys. Rev. X* **9**, 011034 (2019).

[31] T. Fogarty, S. Deffner, T. Busch, and S. Campbell, “Orthogonality catastrophe as a consequence of the quantum speed limit,” *Phys. Rev. Lett.* **124**, 110601 (2020).

[32] K. Suzuki and K. Takahashi, “Performance evaluation of adiabatic quantum computation via quantum speed limits and possible applications to many-body systems,” *Phys. Rev. Research* **2**, 032016 (2020).

[33] A. del Campo, “Probing quantum speed limits with ultracold gases,” *Phys. Rev. Lett.* **126**, 180603 (2021).

[34] R. Hamazaki, “Speed limits for macroscopic transitions,” *PRX Quantum* **3**, 020319 (2022).

[35] S. L. Braunstein, C. M. Caves, and G. J. Milburn, “Generalized uncertainty relations: Theory, examples, and lorentz invariance,” *Annals of Physics* **247**, 135–173 (1996).

[36] V. Giovannetti, S. Lloyd, and L. Maccone, “Advances in quantum metrology,” *Nature Photonics* **5**, 222–229 (2011).

[37] G. Tóth and I. Apellaniz, “Quantum metrology from a quantum information science perspective,” *Journal of Physics A: Mathematical and Theoretical* **47**, 424006 (2014).

[38] M. Beau and A. del Campo, “Nonlinear quantum metrology of many-body open systems,” *Phys. Rev. Lett.* **119**, 010403 (2017).

[39] T. Caneva, M. Murphy, T. Calarco, R. Fazio, S. Montangero, V. Giovannetti, and G. E. Santoro, “Optimal control at the quantum speed limit,” *Phys. Rev. Lett.* **103**, 240501 (2009).

[40] S. An, D. Lv, A. del Campo, and K. Kim, “Shortcuts to adiabaticity by counterdiabatic driving for trapped-ion displacement in phase space,” *Nature Communications* **7**, 12999 (2016).

[41] K. Funo, J.-N. Zhang, C. Chatou, K. Kim, M. Ueda, and A. del Campo, “Universal work fluctuations during shortcuts to adiabaticity by counterdiabatic driving,” *Phys. Rev. Lett.* **118**, 100602 (2017).

[42] S. Campbell and S. Deffner, “Trade-off between speed and cost in shortcuts to adiabaticity,” *Phys. Rev. Lett.* **118**, 100601 (2017).

[43] A. del Campo, J. Goold, and M. Paternostro, “More bang for your buck: Superadiabatic quantum engines,” *Scientific Reports* **4**, 6208 (2014).

[44] F. C. Binder, S. Vinjanampathy, K. Modi, and J. Goold, “Quantacell: powerful charging of quantum batteries,” *New Journal of Physics* **17**, 075015 (2015).

[45] F. Wegner, “Flow-equations for hamiltonians,” *Annalen der Physik* **506**, 77–91 (1994).

[46] S. D. Glazek and K. G. Wilson, “Renormalization of hamiltonians,” *Phys. Rev. D* **48**, 5863–5872 (1993).

[47] S. D. Glazek and K. G. Wilson, “Perturbative renormalization group for hamiltonians,” *Phys. Rev. D* **49**, 4214–4218 (1994).

[48] F. J. Wegner, “Flow equations for hamiltonians,” *Physics Reports* **348**, 77–89 (2001).

[49] S. Kehrein, *The Flow Equation Approach to Many-Particle Systems*, Springer Tracts in Modern Physics (Springer Berlin Heidelberg, 2007).

[50] C. W. von Keyserlingk, T. Rakovszky, F. Pollmann, and S. L. Sondhi, “Operator hydrodynamics, otocs, and entanglement growth in systems without conservation laws,” *Phys. Rev. X* **8**, 021013 (2018).

[51] A. Nahum, S. Vijay, and J. Haah, “Operator spreading in random unitary circuits,” *Phys. Rev. X* **8**, 021014 (2018).

[52] T. Rakovszky, F. Pollmann, and C. W. von Keyserlingk, “Diffusive hydrodynamics of out-of-time-ordered correlators with charge conservation,” *Phys. Rev. X* **8**, 031058 (2018).

[53] V. Khemani, A. Vishwanath, and D. A. Huse, “Operator spreading and the emergence of dissipative hydrodynamics under unitary evolution with conservation laws,” *Phys. Rev. X* **8**, 031057 (2018).

[54] D. E. Parker, X. Cao, A. Avdoshkin, T. Scaffidi, and E. Altman, “A universal operator growth hypothesis,” *Phys. Rev. X* **9**, 041017 (2019).

[55] D. Forster, *Hydrodynamic Fluctuations, Broken Symmetry, And Correlation Functions*, Advanced Books Classics (CRC Press, 2018).

[56] Nicoletta Carabba, Niklas Hörnadal, and Adolfo del Campo, “Quantum speed limits on operator flows and correlation functions,” *Quantum* **6**, 884 (2022).

[57] B. Mohan and A. K. Pati, “Quantum speed limits for observables,” *Phys. Rev. A* **106**, 042436 (2022).

[58] J. L. F. Barbón, E. Rabinovici, R. Shir, and R. Sinha, “On the evolution of operator complexity beyond scrambling,” *Journal of High Energy Physics* **2019**, 264 (2019).

[59] P. Caputa, J. M. Magan, and D. Patramanis, “Geometry of krylov complexity,” *Phys. Rev. Research* **4**, 013041 (2022).

[60] Anatoly Dymarsky and Alexander Gorsky, “Quantum chaos as delocalization in krylov space,” *Phys. Rev. B* **102**, 085137 (2020).

[61] E. Rabinovici, A. Sánchez-Garrido, R. Shir, and J. Sonner, “Operator complexity: a journey to the edge of krylov space,” *Journal of High Energy Physics* **2021**, 62 (2021).

[62] N. Hörnadal, N. Carabba, A. S. Matsoukas-Roubeas, and A. del Campo, “Ultimate speed limits to the growth of operator complexity,” *Communications Physics* **5**, 207 (2022).

[63] H. Mori, “A Continued-Fraction Representation of the Time-Correlation Functions,” *Progress of Theoretical Physics* **34**, 399–416 (1965).

[64] R. Kubo, “The fluctuation-dissipation theorem,” *Reports on Progress in Physics* **29**, 255 (1966).

[65] G. Müller V. S. Viswanath, *The Recursion Method: Application to Many-Body Dynamics* (Springer-Verlag, 1994).

[66] R. R. Ernst, G. Bodenhausen, and A. Wokaun, *Principles of Nuclear Magnetic Resonance in One and Two Dimensions*, International series of monographs on chemistry (Clarendon Press, 1990).

[67] J. A. Gyamfi, “Fundamentals of quantum mechanics in liouville space,” *European Journal of Physics* **41**, 063002 (2020).

[68] S. H. Friedberg, A. J. Insel, and L. E. Spence, *Linear Algebra* (Pearson, 2019).

[69] L. B. Levitin and T. Toffoli, “Fundamental limit on the rate of quantum dynamics: The unified bound is tight,” *Phys. Rev. Lett.* **103**, 160502 (2009).

[70] J. Haegeman, T. J. Osborne, H. Verschelde, and F. Verstraete, “Entanglement renormalization for quantum fields in real space,” *Phys. Rev. Lett.* **110**, 100402 (2013).

[71] M. Nozaki, S. Ryu, and T. Takayanagi, “Holographic geometry of entanglement renormalization in quantum field theories,” *Journal of High Energy Physics* **2012**, 193 (2012).

[72] J. Molina-Vilaplana and A. del Campo, “Complexity functionals and complexity growth limits in continuous mera circuits,” *Journal of High Energy Physics* **2018**, 12 (2018).

[73] P. Caputa, N. Kundu, M. Miyaji, T. Takayanagi, and K. Watanabe, “Anti-de sitter space from optimization of path integrals in conformal field theories,” *Phys. Rev. Lett.* **119**, 071602 (2017).

[74] P. Caputa, N. Kundu, M. Miyaji, T. Takayanagi, and K. Watanabe, “Liouville action as path-integral complexity: from continuous tensor networks to ads/cft,” *Journal of High Energy Physics* **2017**, 97 (2017).

[75] A. R. Brown, D. A. Roberts, L. Susskind, B. Swingle, and Y. Zhao, “Complexity, action, and black holes,” *Phys. Rev. D* **93**, 086006 (2016).

[76] A. R. Brown, D. A. Roberts, L. Susskind, B. Swingle, and Y. Zhao, “Holographic complexity equals bulk action?” *Phys. Rev. Lett.* **116**, 191301 (2016).

[77] R. Uzdin and R. Kosloff, “Speed limits in liouville space for open quantum systems,” *EPL (Europhysics Letters)* **115**, 40003 (2016).

[78] D. A. Lidar, A. Shabani, and R. Alicki, “Conditions for strictly purity-decreasing quantum markovian dynamics,” *Chemical Physics* **322**, 82–86 (2006).

[79] M. Toda, “Vibration of a chain with nonlinear interaction,” *Journal of the Physical Society of Japan* **22**, 431–436 (1967).

[80] M. Toda, “Wave propagation in anharmonic lattices,” *Journal of the Physical Society of Japan* **23**, 501–506 (1967).

[81] H. Flaschka, “The toda lattice. ii. existence of integrals,” *Phys. Rev. B* **9**, 1924–1925 (1974).

[82] J. Moser, *Dynamical Systems, Theory and Applications* (Springer, 1975).

[83] C. Monthus, “Flow towards diagonalization for many-body-localization models: adaptation of the toda matrix differential flow to random quantum spin chains,” *Journal of Physics A: Mathematical and Theoretical* **49**, 305002 (2016).

[84] M. Okuyama and K. Takahashi, “From classical nonlinear integrable systems to quantum shortcuts to adiabaticity,” *Phys. Rev. Lett.* **117**, 070401 (2016).

[85] D. Chowdhury, A. Georges, O. Parcollet, and S. Sachdev, “Sachdev-ye-kitaev models and beyond: Window into non-fermi liquids,” *Rev. Mod. Phys.* **94**, 035004 (2022).

[86] S. Bravyi, D. P. DiVincenzo, and D. Loss, “Schrieffer–wolff transformation for quantum many-body systems,” *Annals of Physics* **326**, 2793–2826 (2011).

[87] L. D. Faddeev and L. A. Takhtajan, *Hamiltonian Methods in the Theory of Solitons* (Springer, Berlin Heidelberg, 2007).

[88] B. Sutherland, *Beautiful Models* (World Scientific, 2004).

[89] D. J. Gross, J. Kruthoff, A. Rolph, and E. Shaghoulian, “ $t\bar{T}$ in ads_2 and quantum mechanics,” *Phys. Rev. D* **101**, 026011 (2020).

[90] D. J. Gross, J. Kruthoff, A. Rolph, and E. Shaghoulian, “Hamiltonian deformations in quantum mechanics, $t\bar{T}$, and the syk model,” *Phys. Rev. D* **102**, 046019 (2020).

[91] A. S. Matsoukas-Roubeas, F. Roccati, J. Cornelius, Z. Xu, A. Chenu, and A. del Campo, “Non-hermitian hamiltonian deformations in quantum mechanics,” (2022).

- [92] A. Bhattacharya, P. Nandy, P. P. Nath, and H. Sahu, “Operator growth and krylov construction in dissipative open quantum systems,” *Journal of High Energy Physics* **2022**, 81 (2022).
- [93] C. Liu, H. Tang, and H. Zhai, “Krylov complexity in open quantum systems,” (2022).